STRESS ANALYSIS OF TRANSVERSE SHIP FRAMES

LOWELL P. DANIELS
WARD J. DAVIES

Thesis
D15

Library
U. S. Naval Postgraduate School
Monterey, California

Mont 115
8854

STRESS ANALYSIS OF TRANSVERSE SHIP FRAMES

by

Lowell P. Daniels
Lieutenant Commander,
United States Navy,
B.B.A., University
of Minnesota, 1941

Ward J. Davies, Jr.
Lieutenant, U. S. Coast
Guard, B.S., U.S.
Coast Guard Academy,
1943

Submitted in Partial Fulfillment of the Requirements

for the Degree of

NAVAL ENGINEER

from the

MASSACHUSETTS INSTITUTE OF TECHNOLOGY

1950

Thesis
D15

DUDLEY KNOX LIBRARY
NAVAL POSTGRADUATE SCHOOL
MONTEREY, CALIFORNIA 93940

Cambridge, Massachusetts
May 19, 1950

Professor J. S. Newell,
Secretary of the Faculty,
Massachusetts Institute of Technology,
Cambridge, Massachusetts.

Dear Sir:

In accordance with the requirements for the Degree of Naval Engineer, we submit herewith a thesis entitled, "Stress Analysis of Transverse Ship Frames."

Respectfully,

ACKNOWLEDGEMENT

The authors wish to express their sincere appreciation and indebtedness to Professor Charles H. Norris for his suggestion of the thesis topic and his patient guidance during the investigation.

Both authors are also grateful to Prof. J. H. Evans for his advice and to Prof. George C. Manning for the use of his elaboration of Hovgaard's Closed Frame Ring Method.

TABLE OF CONTENTS

	Page
Summary	1
Introduction	3
Procedure	5
Results	8
Discussion of Results	14
Conclusions	18
Recommendations	19
Appendix	20
A. Description of Assumptions and Formulation of the Characteristics of the Frame	21
B. Description of the Model Design, Manufacture and Testing Procedure	27
C. Calculation of Influence Lines by the Elastic Center Method	37
D. Calculation of Influence Lines by the Hovgaard Method	54
E. Original Data	70
F. Bibliography	78

SUMMARY

Object:

The purpose of this investigation was to compare the results of two theoretical methods of calculating stress in a ship's transverse frame with an experimental model analysis.

Procedure:

The experimental stress analysis for a ship's frame was made using a planar celluloid model and the Beggs method. Calculations were made using the elastic center method based on the law of virtual work and the method of Prof. K. Hovgaard to determine influence lines of stress due to vertical and horizontal unit loads. The results were compared using the experimental results as a basis of comparison.

Results:

The families of six influence lines obtained by each of the three methods of analysis agreed very closely.

Conclusions:

The experimental results verified that the methods of calculation of stress using twelve integration stations gave consistent accuracy. The elastic center method required less

computation work and attained a slightly greater degree of accuracy.

Recommendations:

It is recommended that further work be undertaken (1) to determine the amount of error resulting from the simplifying assumptions used and (2) to obtain a similar comparison for a ship with two or more decks. The simplifying assumptions were that the moment of inertia varied as a continuous function and that the effects of axial force and shear were negligible. Further model analysis should be made using models that have a greater degree of stiffness to better overcome frictional forces.

Introduction

The determination of stress in the transverse frame of a ship presents a difficult problem because of the complicated structure involved. A number of methods of solution have been devised. Mr. J. Bruhn in reference (2) proposed a method based on Castigliano's principle of least work. Prof. A. A. Howard gave a method based on deflections in reference (5). In addition to those methods advanced by naval architects, other methods applicable to any structure in the form of a closed ring are available. One of these is the application of the law of virtual work frequently used by civil engineers for indeterminate structures.

The above methods are all based on mathematical hypothesis and are completely accurate only if the mathematical expressions used exactly represent the actual structure. This is impractical for the ship frame, and simplifying assumptions are necessary in order to make the computation possible in a reasonable amount of time. The work of integration in the theoretical methods is reduced by using as few stations as possible consistent with reasonable accuracy. The actual moment of inertia varies abruptly and frequently, but it is generally assumed to be represented by a continuous curve faired through the several values. This curve will not necessarily correspond to the actual change in the moment

of inertia and thus a discrepancy from the actual moment of inertia may exist at the point represented. A second assumption usually made is that the effects of axial and sheer distortion are small relative to that of the bending distortion and are neglected.

This investigation determines the influence lines for each of the redundant forces due to unit vertical and horizontal loads. These influence lines are determined experimentally and theoretically by two methods. The two theoretical methods are compared to the experimental results and evaluated for accuracy and ease of computation.

The apparatus used to determine the influence lines experimentally consisted of a planar celluloid model which had a moment of inertia proportional to the actual ship frame. The frame was cut at the keel and a Berys deformeter gage installed which produced distortions of a known magnitude. The deflections produced by these distortions at selected points were then measured with a micrometer microscope. The ordinates of the influence line for a load applied at these points are then determined by application of the Muller-Breslau principle.

One of the theoretical methods of determining the influence lines consists of utilizing the law of virtual work with the redundants located at the elastic center. The other is the method of Prof. Hovgaard as described in reference (5).

PROCEDURE

The procedure used in this investigation for determining the influence lines consisted of four parts (1) setting the conditions of the problem and determining the data necessary for the experimental and theoretical methods of analysis (2) manufacture of the model and performance of experimental work (3) calculation by the method of virtual work using the elastic center and (4) calculation by the Hovgaard method.

A transverse frame of a modern destroyer, which is typical of naval construction, was selected as the source of all data. The moment of inertia and distance of the neutral axis from the molded line were determined at twenty-five points. This relatively large number of points was used in order to make the values of moment of inertia approximate the actual frame as closely as possible. Large-scale curves were plotted of moment of inertia versus distance along the molded girth and of neutral axis distance from molded line versus distance along the molded girth. The coordinates of points on the neutral axis were determined graphically from a drawing of the molded line. Appendix A describes in more detail how the fundamental data were obtained.

A planar model, having the shape of the neutral axis and moment of inertia proportional to that of the prototype, was made. It was cut from a sheet of celluloid and filed

until the depth gave the required moment of inertia. The method of calculating the model dimensions and the actual micrometer measurements obtained may be found in Appendix B. Next the frame was cut at the location of the keel and the ends clamped into the two halves of a Beggs deformeter gage. The right half of the gage was screwed to the table.

Briefly the experimental work consisted of introducing known distortions into the model structure and measuring the deflection of each point at which an influence line ordinate was desired. Distortions of a known magnitude are introduced by inserting the various sizes of calibrated plugs into the Beggs deformeter gage. The horizontal deflection of a point measured by the microscope gives the data for determining the ordinate to the influence line of a redundant due to a unit horizontal load. Similarly the vertical deflection gives the data for the influence line of a redundant due to a unit load applied vertically. The ordinate of the influence line for a redundant is equal to minus one times the ratio of the measured deflection to the introduced deflection. The deflection for each of 24 points around the frame was measured to determine each influence line. Due to symmetry of the structure only the 12 readings for one side of the model are necessary; however, the other readings may be used as a check. The details of the experimental work are explained more fully in Appendix B.

The influence line for each redundant force was calculated by the method of virtual work with the location of the redundants at the elastic center. The location of the redundants at this point eliminates the solution of simultaneous equations. For comparison with the redundants determined experimentally the redundants at the elastic center were transferred to the same location. The details of the calculation by the elastic center method are given in Appendix C.

The other method of calculation utilized the method of the late Prof. N. Hovgaard to determine the influence lines for each redundant. This method requires the solution of simultaneous equations. The calculation details are given in Appendix D.

RESULTS

The results of this investigation consist of the influence line ordinates for moment, thrust and shear caused by unit vertical and horizontal loads. The results are tabulated and compared in Tables I and II.

Small-scale plots of the results are shown in Figures I, II, and III. The curves represent the values found by all three methods. To plot the results of all methods would require too large a scale to be practical. The results are best compared in tabular form.

Figure VI is an aid in visualizing the significance of the results.

Table I

Comparison of Influence Lines for Redundants due to Unit Vertical Load

	Experimental Result			By Elastic Center			Amt. Diff. from Exp.			Percent Diff.		
Stat.	X_1	X_2	X_3	X_1'	X_2'	X_3'	X_1-X_1'	X_2-X_2'	X_3-X_3'	X_1'	X_2'	X_3'
0	0	0	-1.0000	0	0	-1.0000	0	0	0	0	0	0
1	- 4.1099	-.0048	- .9797	- 4.1574	-.0042	-1.0000	.0475	.0006	.0203	1.16	12.76	2.07
2	- 7.7548	-.0307	- .9844	- 7.9146	-.0289	-1.0017	.1598	.0018	.0173	2.06	5.98	1.75
3	-11.6133	-.0650	- .9917	-11.2609	-.0631	-1.0052	.2476	.0020	.0135	2.25	3.03	1.36
4	-13.4206	-.1294	- .9885	-13.6439	-.1250	-1.0170	.2233	.0044	.0285	1.66	3.42	2.88
5	-14.8800	-.1763	-1.0137	-15.0147	-.1761	-1.0292	.1347	.0002	.0155	.91	.11	1.53
6	-15.3986	-.2068	-1.0688	-15.5065	-.2066	-1.0400	.1080	.0002	.0289	.70	.11	2.70
7	-15.5102	-.2233	-1.0363	-15.6364	-.2168	-1.0443	.1262	.0065	.0080	.81	2.93	.77
8	-15.1411	-.2218	-1.0213	-15.5643	-.2219	-1.0467	.4232	.0001	.0254	2.80	.05	2.49
9	-13.7819	-.1096	- .9403	-13.9709	-.1067	- .9486	.1890	.0034	.0083	1.37	3.09	.88
10	-11.8038	-.0259	- .7971	-11.7890	-.0228	- .8034	.0148	.0031	.0063	.13	12.01	.79
11	- 9.4753	+.0314	- .6468	- 9.6125	+.0331	- .6569	.1372	.0017	.0101	1.45	5.25	1.56
12	- 7.3541	+.0446	- .4867	- 7.1536	+.0432	- .5000	.2005	.0014	.0133	2.73	3.05	2.73

	By Hovgaard Method											
	X_1	X_2	X_3	X_1''	X_2''	X_3''	X_1-X_1''	X_2-X_2''	X_3-X_3''	X_1''	X_2''	X_3''
0	0	0	-1.0000	0	0	-1.0000	0	0	0	0	0	0
1	- 4.1099	-.0048	- .9797	- 4.1573	-.0042	-1.0000	.0474	.0006	.0203	1.15	12.76	2.07
2	- 7.7548	-.0307	- .9844	- 7.9143	-.0289	-1.0017	.1595	.0019	.0173	2.06	6.08	1.75
3	-11.0133	-.0650	- .9917	-11.2604	-.0631	-1.0051	.2509	.0019	.0134	2.35	2.97	1.36
4	-13.4206	-.1294	- .9885	-13.6426	-.1251	-1.0170	.2220	.0043	.0285	1.65	3.36	2.88
5	-14.8800	-.1763	-1.0137	-15.0279	-.1762	-1.0291	.1479	.0001	.0155	.99	.02	1.53
6	-15.3986	-.2068	-1.0688	-15.5026	-.2069	-1.0400	.1040	.0001	.0289	.68	.02	2.70
7	-15.5102	-.2233	-1.0363	-15.6340	-.2169	-1.0442	.1237	.0064	.0079	.80	2.86	.76
8	-15.1411	-.2218	-1.0213	-15.5619	-.2221	-1.0467	.4208	.0003	.0254	2.78	.12	2.48
9	-13.7819	-.1096	- .9403	-13.9875	-.1052	- .9486	.2057	.0044	.0083	1.49	4.05	.88
10	-11.8038	-.0259	- .7971	-11.8278	-.0203	- .8034	.0240	.0056	.0063	.20	21.55	.79
11	- 9.4753	+.0314	- .6468	- 9.6724	+.0369	- .6569	.1971	.0055	.0101	2.08	17.41	1.56
12	- 7.3541	+.0446	- .4867	- 7.2348	+.0484	- .5000	.1194	.0038	.0133	1.62	8.56	2.73

Table II

Comparison of Influence Lines for Redundants due to Unit Horizontal Load

	Experimental Result			By Elastic Center			Amt. Diff. from Exp.			Percent Diff.		
Stat.	X_1	X_2	X_3	X_1'	X_2'	X_3'	X_1-X_1'	X_2-X_2'	X_3-X_3'	X_1'	X_2'	X_3'
0	0	-1.0000	0	0	-1.0000	0	0	0	0	0	0	0
1	.6295	- .9979	.0058	.6079	- .9994	0	.0216	.0015	.0058	3.43	.15	100.00
2	1.4022	- .9852	.0024	1.3700	- .9944	.0003	.0322	.0092	.0021	2.30	.93	85.95
3	2.4761	- .9800	.0049	2.3605	- .9843	.0014	.1156	.0042	.0036	4.67	.43	72.25
4	3.6630	- .9464	.0051	3.5285	- .9461	.0087	.1658	.0003	.0035	4.53	.03	69.33
5	5.7732	- .8060	.0281	5.8443	- .8717	.0264	.0712	.0057	.0018	1.23	.70	6.27
6	7.5187	- .7579	.0694	7.5911	- .7592	.0662	.0724	.0013	.0033	.96	.17	4.71
7	9.3358	- .6197	.1257	9.1928	- .6369	.1182	.1430	.0172	.0075	1.53	2.78	5.99
8	10.6306	- .5225	.1955	10.6638	- .5174	.1915	.0372	.0051	.0040	.35	.98	2.05
9	10.7057	- .5247	.1997	10.8139	- .5073	.2002	.1082	.0174	.0005	1.01	3.31	.25
10	10.6854	- .5193	.1973	10.9416	- .5025	.2086	.0562	.0168	.0113	.52	3.23	5.72
11	10.9668	- .5021	.2054	11.0067	- .5009	.2130	.0399	.0012	.0076	.36	.24	3.70
12	11.0670	- .4988	.2112	11.0361	- .5007	.2148	.0309	.0019	.0076	.28	.39	3.69

By Hovgaard Method

	X_1	X_2	X_3	X_1''	X_2''	X_3''	X_1-X_1''	X_2-X_2''	X_3-X_3''	X_1''	X_2''	X_3''
0	0	-1.0000	0	0	-1.0000	0	0	0	0	0	0	0
1	.6295	- .9979	.0058	.6079	- .9994	0	.0216	.0015	.0058	3.44	.15	100.0
2	1.4022	- .9852	.0024	1.3699	- .9944	.0003	.0323	.0092	.0021	2.30	.93	85.95
3	2.4761	- .9800	.0049	2.3604	- .9843	.0014	.1157	.0042	.0036	4.67	.43	72.25
4	3.6630	- .9464	.0051	3.5280	- .9461	.0087	.1652	.0003	.0034	4.51	.03	69.33
5	5.7732	- .8060	.0281	5.8898	- .8741	.0264	.1166	.0080	.0018	2.02	.93	6.34
6	7.5187	- .7579	.0694	7.5891	- .7590	.0661	.0704	.0011	.0033	.94	.15	4.77
7	9.3358	- .6197	.1257	9.1879	- .6366	.1181	.1479	.0169	.0076	1.58	2.72	6.04
8	10.6306	- .5225	.1955	10.6564	- .5169	.1914	.0258	.0056	.0041	.24	1.07	2.08
9	10.7057	- .5247	.1997	10.8063	- .5067	.2001	.1006	.0180	.0004	.94	3.42	.21
10	10.6854	- .5193	.1973	10.9312	- .5018	.2065	.0458	.0175	.0112	.42	3.36	5.69
11	10.9668	- .5021	.2054	10.9957	- .5001	.2129	.0289	.0020	.0075	.26	.39	3.67
12	11.0670	- .4988	.2112	11.0248	- .5000	.2148	.0422	.0012	.0076	.38	.23	3.66

FIGURE I

INFLUENCE LINE FOR BENDING MOMENT AT STATION 0

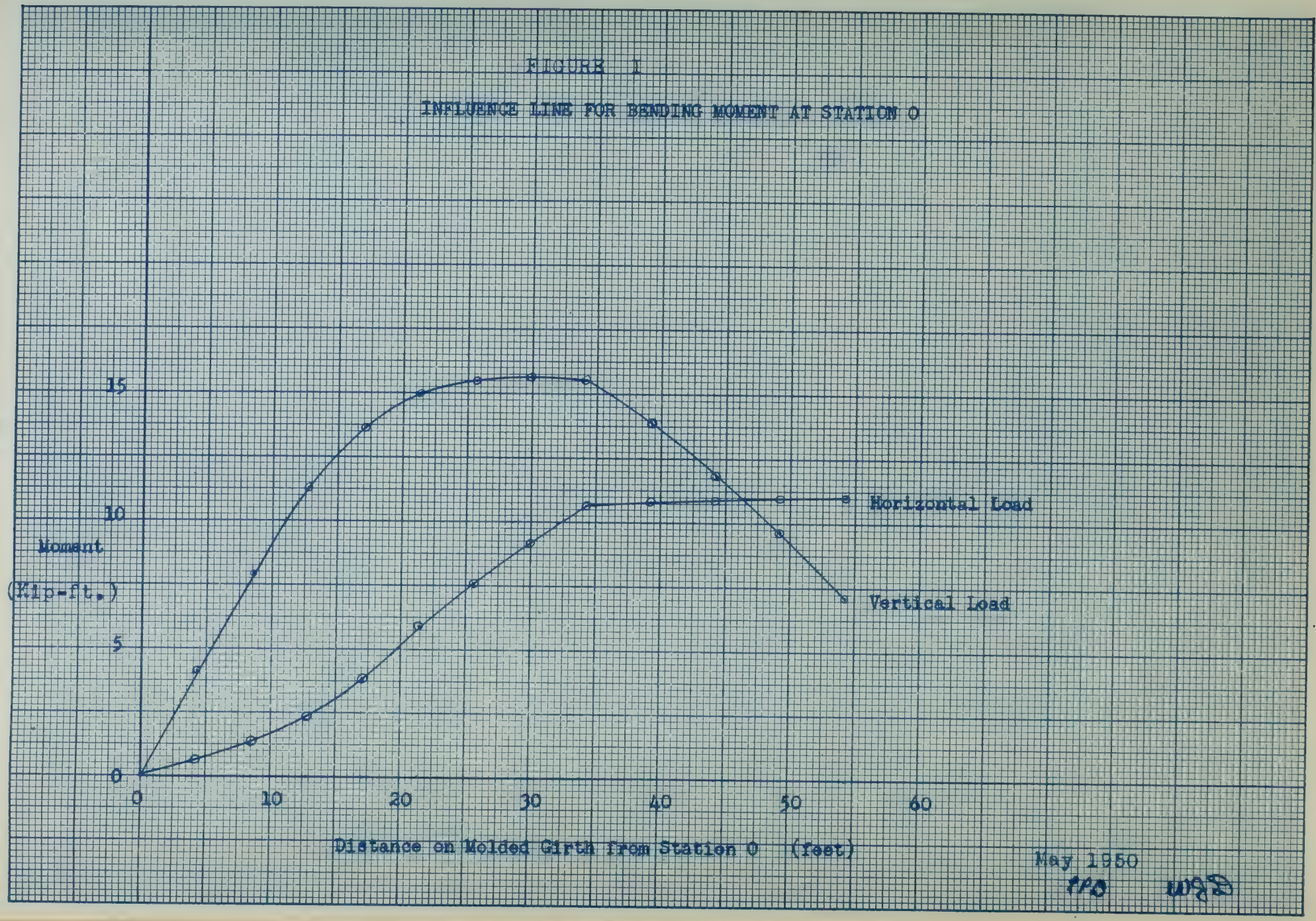

May 1950

FIGURE II

INFLUENCE LINE FOR THRUST AT STATION 0

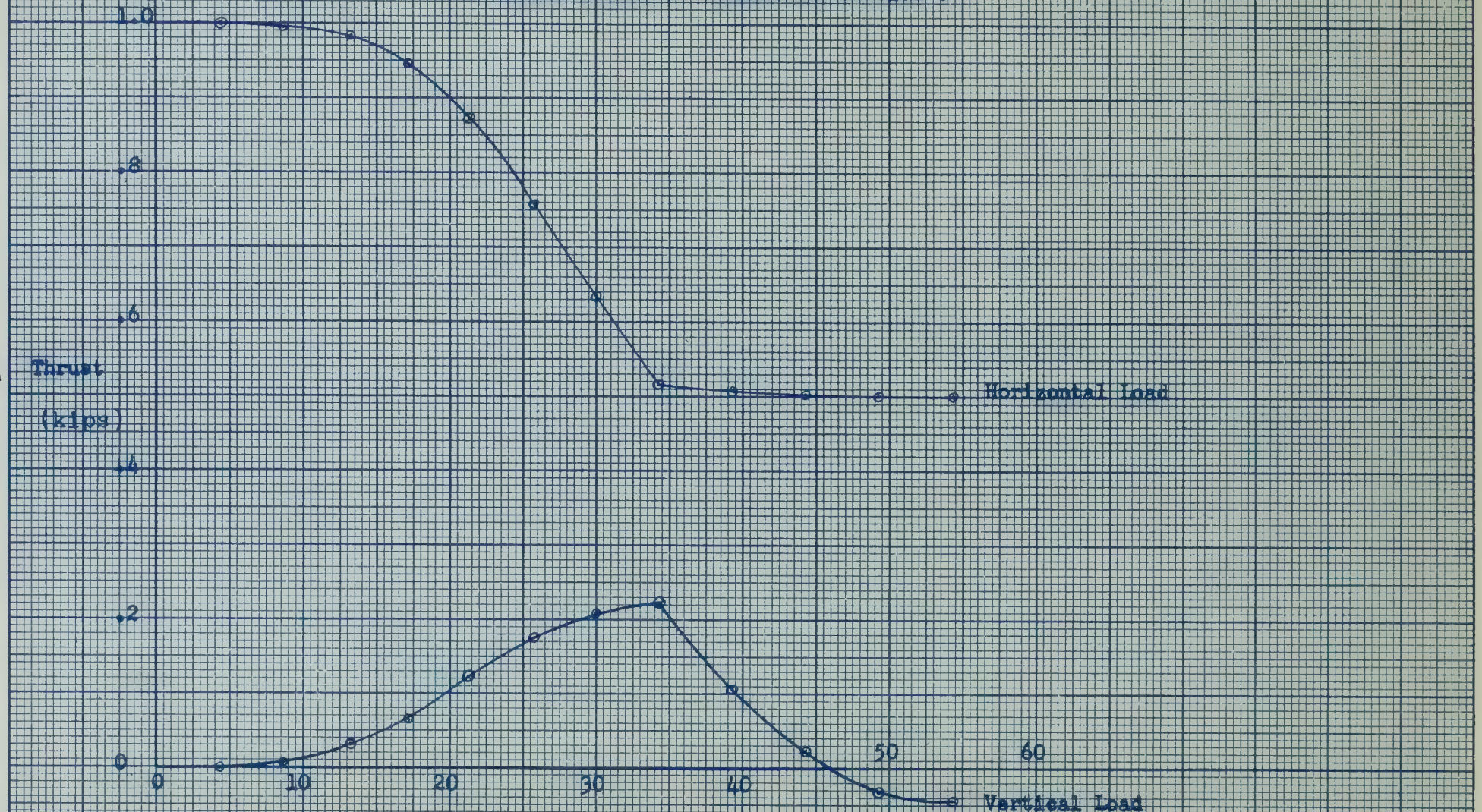

May 1950

FIGURE III

INFLUENCE LINE FOR SHEAR AT STATION 0

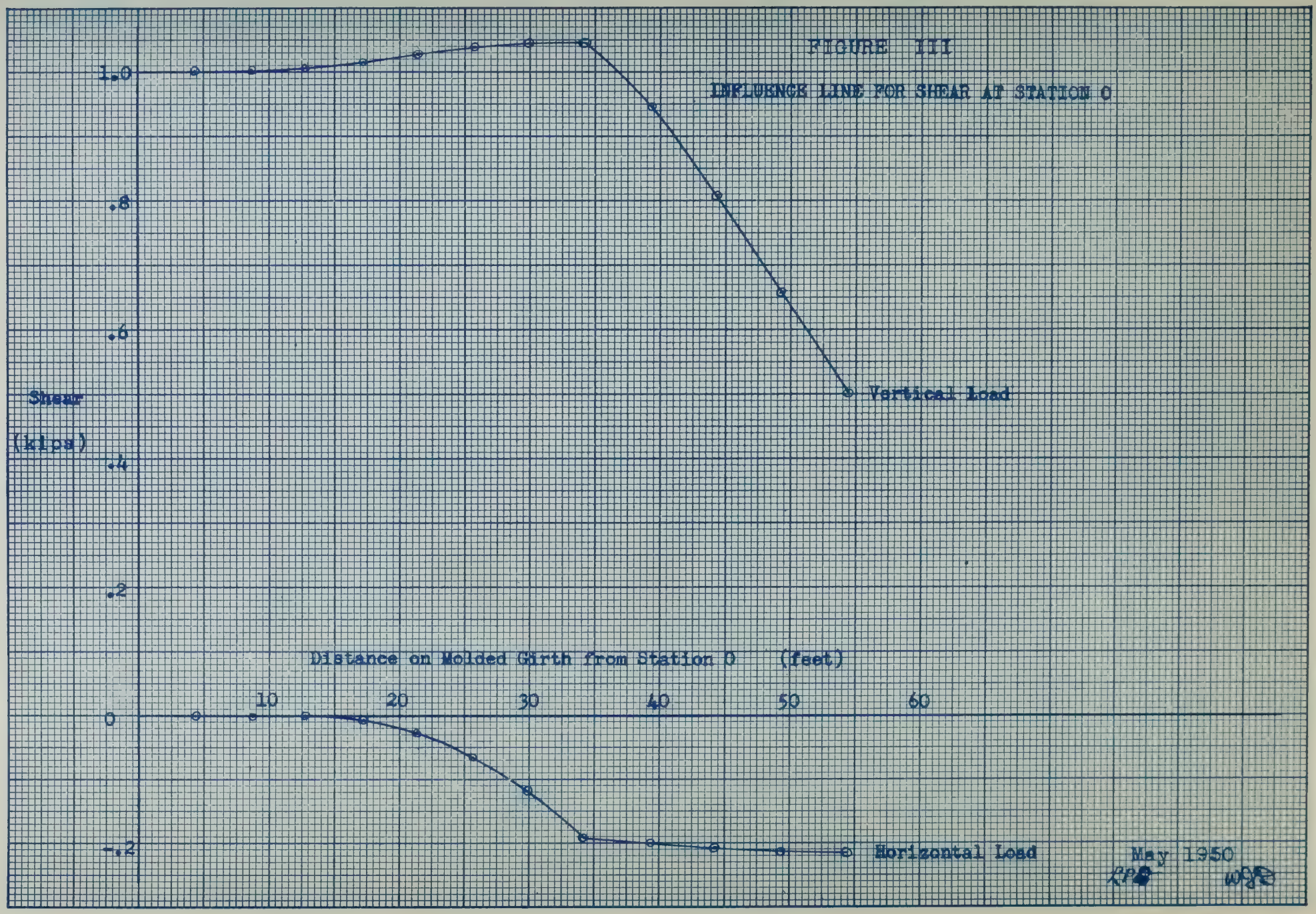

May 1950

DISCUSSION OF RESULTS

The three methods of obtaining the influence lines given in tables I and II show very good agreement. For purposes of comparison the influence line determined experimentally was selected as a base.

Experimental techniques are always subject to measurement errors and to physical phenomena beyond the control of the experimenters. Every effort was made to minimize these types of errors. The principal errors applicable to this investigations are listed below:

(1) Friction forces in the model mounting apparatus of sufficient magnitude to prevent normal deflection.

(2) Alignment errors in mounting the model in the Beggs apparatus and in orienting the microscope.

(3) Uncertainty of microscope readings because of personal observation errors.

(4) Error in the calibration constant obtained for the microscope.

(5) Errors in the introduced distortions caused by the Beggs plugs not being the stated size by ±0.0001".

(6) Errors in the model manufacture where the filed depth differed from the theoretical. These destroyed strict proportionality between the model and prototype moment of inertia.

(7) Variations in the modulus of elasticity due to non-homogeneity of the model material.

(8) Distortions of the model due to localized thermal expansions.

The authors estimate the cumulative effect of the above errors to be 12 microscope units. The probable error incurred will only be 5 microscope units. This error will affect the thrust and shear redundants by the amount of ±.0183 and the moment redundant by ±.179. Thus in Tables I and II any differences between the experimental and the calculated results which are of smaller magnitude lie within the probable experimental error. It is noted that nearly all the high percentage errors occur where the magnitude of the readings is very small and could be due entirely to this cause. Considering the differences of results which are outside the magnitude of the experimental error the maximum percentage difference was 2.86%.

The two methods of calculating the influence lines should have given identical results since they are both based on correct mathematical theories and the same basic data were used for each method. The disagreement between the results of the two methods can be attributed to: (1) solution of simultaneous equations in the Hovgaard method, (2) transfer of redundants from one location to another, and (3) errors in computation. The equations obtained by the Hovgaard method

are those of straight lines with a very small angle of intersection. This poorly defined intersection makes it possible to obtain several different values depending on the procedure used in eliminating variables during the solution of the simultaneous equations. The procedure followed in this investigation minimised this error although it could still be detected. Transfer of redundants caused magnification of any small errors that existed to a size where they could become significant. This additional step was taken for the sole purpose of making the redundants alike and would normally not be necessary. Arithmetical errors in computations of this magnitude are difficult to eliminate completely but the authors have made exhaustive checks and feel assured that none exist.

The remainder of the discrepancy between the theoretical and experimental solutions may be attributed to the more accurate integration of effects by the model and the neglect of axial stress and shear effects in the computations. The model was constructed with the moment of inertia proportional to the prototype at 41 points while only 12 points were used in the computations. This difference would tend to make the model results more accurate. Axial stress and shear stress effects are entirely neglected in the computations while in the model they are partially taken into account. The effect cannot be considered comparable to that in the prototype because the cross sectional shapes are not similar.

The work of computation by the elastic center method was found to be slightly less than for the Hovgaard method. The amount of computation was nearly equal for both in the initial and intermediate parts of the work. However the last part of the Hovgaard method consists of the solution of simultaneous equations which take appreciably longer than the divisions in the last part of the elastic center method.

The solution of stress in a transverse ship's frame may be obtained by the use of influence lines as in this investigation if desired. Solution by means of influence lines is approximately five times more work of computation than a direct singular solution for a specific loading system. However the influence lines can be determined by a mechanical procedure once a form is set up for any given type of frame, and plotting the ordinates provides a ready means of detecting errors in the computation. Influence lines can be used for any system of loading without change and therefore are flexible for determining changes in loading systems. The choice of influence lines over a singular solution will depend on the value attached to the above factors in any particular case.

CONCLUSIONS

1. Experimental analysis verifies that calculation of the indeterminate redundants by either the elastic center or Hovgaard methods is accurate to about 3 per cent for this type of frame if only 12 integration stations are used.

2. The elastic center method requires somewhat less time for calculation than the Hovgaard method because of the elimination of simultaneous equations.

3. In the Hovgaard method the simultaneous equations that must be solved are quite sensitive to small errors which may reduce the accuracy.

4. The Beggs method of experimental analysis can be relied on for good results and requires only models that are inexpensive and easy to make.

5. Plotting influence lines provides a check on the accuracy of the results.

6. Influence lines provide a more satisfactory solution than a singular solution for a specific loading system under certain circumstances.

RECOMMENDATIONS

1. It is recommended that an investigation be made to determine the amount of error resulting from the simplifying assumptions that the moment of inertia varies as a continuous function and that the effects of axial stress and shear stress are negligible.

2. This investigation should be extended to the case of a ship having two or more decks. It is expected that the elastic center method for computing stress will prove to have a more marked superiority over the Hovgaard method than was shown in this investigation.

3. To increase the accuracy, by reducing the frictional effects, a stiffer model should be used. The frame could be stiffened by increasing the thickness of the material, by increasing the depth of the frame, or reducing the scale of the linear dimensions.

A P P E N D I X

APPENDIX A

Description of Assumptions and Formulation of the Characteristics of the Frame

As a basis for analysis a transverse ship frame representative of naval construction was desired. Transverse frame 141 1/7 of the DD692 class destroyer, BuShips Plan No. 565652, was arbitrarily selected for study. In the analysis of this frame the following assumptions are made:

(1) The moment of inertia of the frame is not affected by the longitudinals, lightening holes, or cable runs that pierce the web.

(2) One frame space of shell plating is considered to be effective. This is in accordance with the U.S. Navy practice as given in Bureau of Ships Memorandum No. 447.

(3) The shell plating is assumed to lie on the molded line as it would with welded construction. With the actual type of in and out plating used in this frame the neutral axis was found to vary by as much as 0.603". In order to avoid a discontinuity in the neutral axis some correction was necessary. It was done by this assumption so as to avoid considering a greater moment of inertia than exists at any point. The error is on the conservative side.

(4) The frame was considered to be symmetrical on the

port and starboard sides.

The moment of inertia and the distance of the neutral axis from the molded line for this frame were calculated at 25 points along one half the girth. This relatively large number of points was used so the data would more closely approximate the conditions of the actual frame. The results of this calculation are shown in Table III. From these results large-scale plots were made of moment of inertia vs. distance along one half the girth of the molded line and the neutral axis distance from the molded line vs. distance along one half the girth of the molded line. Small-scale copies of these curves are shown in Figures IV and V respectively.

The offsets representing the shape of the neutral axis were obtained in the following manner. A large-scale drawing of the molded line was made. On this was constructed the neutral axis from distances read from Figure V. Twelve stations were selected for use in the calculations to give the usual degree of accuracy. It was desirable that one station be located at the deck edge because of a possible discontinuity. To do this the deck was divided into four equally spaced stations of 5.031 ft. The side shell was divided into eight equally spaced stations of 4.285 ft. These 12 points were located on the neutral axis and the offsets obtained. These are given in Table IV.

Table III
Moment of Inertia and Neutral Axis
Distance from Molded Line on Prototype

Station	I in^4	C in
0	1201.470	4.348
1	959.782	4.661
2	959.782	4.661
3	896.714	5.026
4	775.415	4.625
5	511.364	4.032
6	484.003	3.905
7	423.970	4.590
8	412.114	4.516
9	394.694	4.410
10	377.682	4.303
11	350.306	4.128
12	329.239	3.988
13	396.971	1.678
14	377.692	1.620
15	352.859	1.543
16	277.395	1.224
17-25	253.118	1.914

FIGURE IV

MOMENT OF INERTIA
VS.
DISTANCE ALONG MOLDED GIRTH

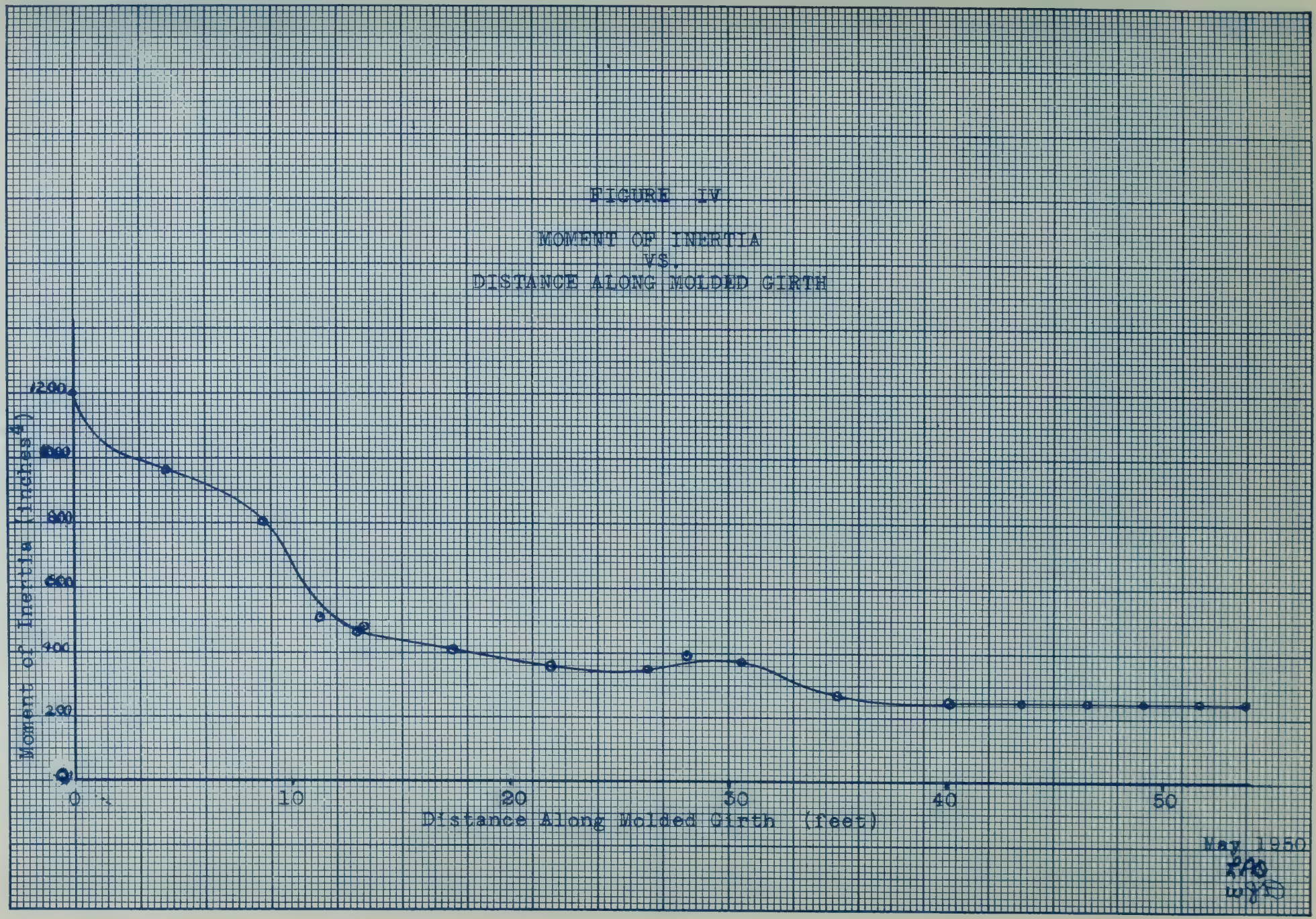

May 1950

FIGURE V

NEUTRAL AXIS DISTANCE FROM MOLDED LINE
Vs.
DISTANCE ALONG MOLDED GIRTH

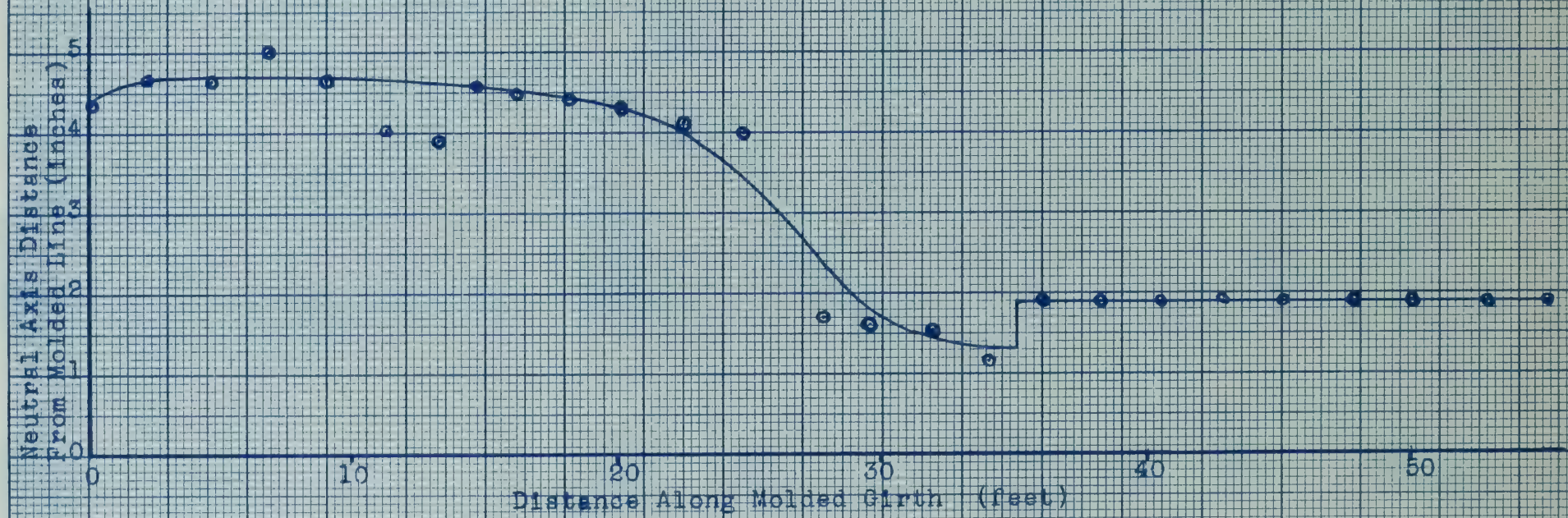

May 1950

FIGURE VI

DRAWING OF NEUTRAL AXIS SHOWING LOCATION OF STATIONS

(Scale 1" = 5'-0")

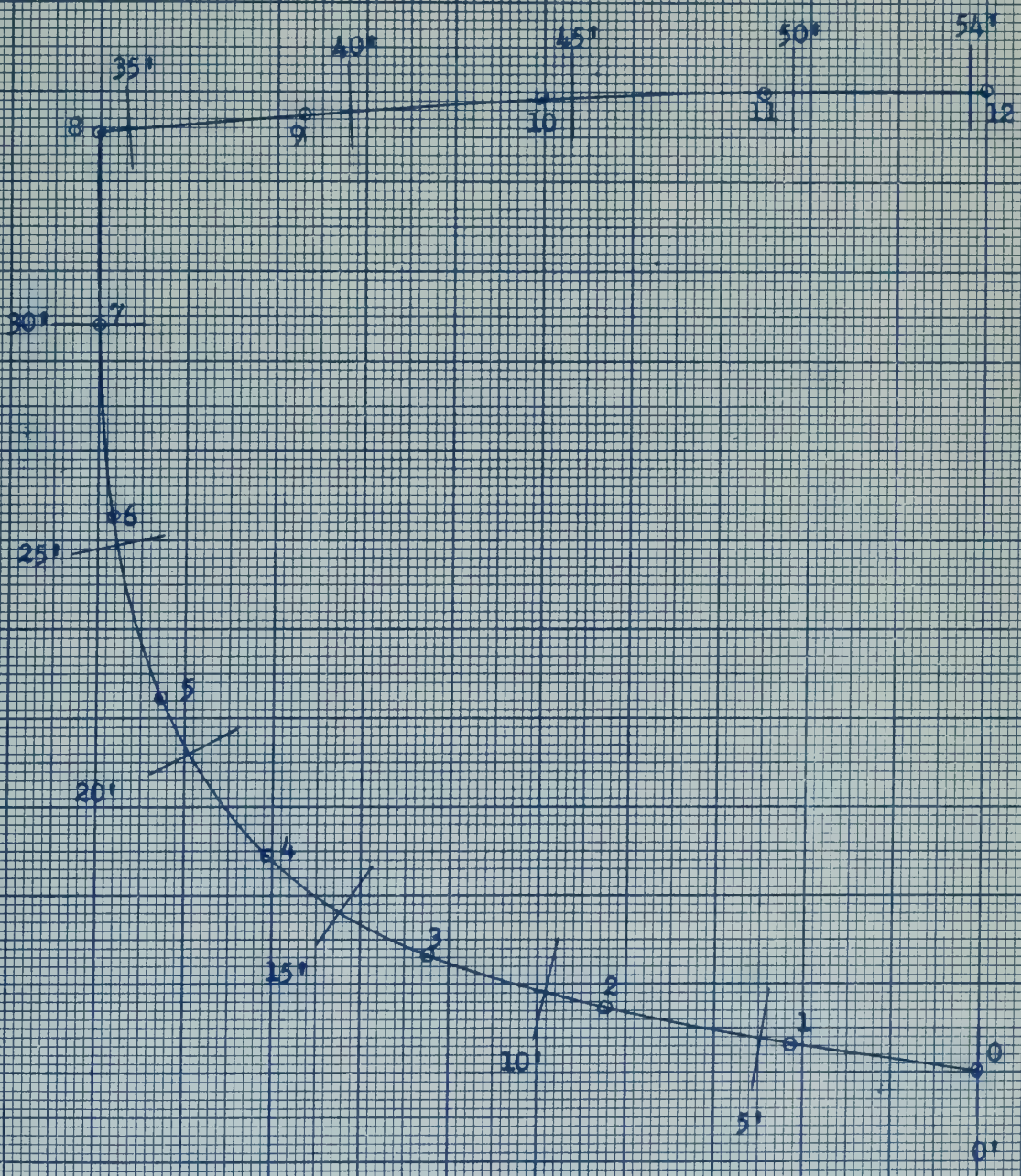

May 1950

APPENDIX B

Description of the Model Design, Manufacture, and Testing Procedure for Obtaining Influence Lines of the Redundants

Theoretical Principle

The determination of influence lines for redundants by experimental means is based on the Müller-Breslau principle. This principle states:

> The ordinates of the influence line for any stress element (such as axial stress, shear, or moment) of any structure are proportional to those of the deflection curve which is obtained by removing the restraint corresponding to that element from the structure and introducing in its place a deformation into the primary structure which remains.[1]

Prof. G. E. Beggs has developed a method and the necessary equipment for application of the Müller-Breslau principle to the analysis of structures. The equipment consists of a model of the structure, a Beggs deformeter gage, and a micrometer microscope. The Beggs method is fully described in references (1) and (6). Its application to this investigation will be discussed under the testing procedure of the model.

The development of the application of this principle follows. Consider the axial thrust developed during application

---

1. Wilbur, J. B. and C. H. Norris, Elementary Structural Analysis, McGraw-Hill Book Co., New York, 1948, p. 450.

FIGURE VII

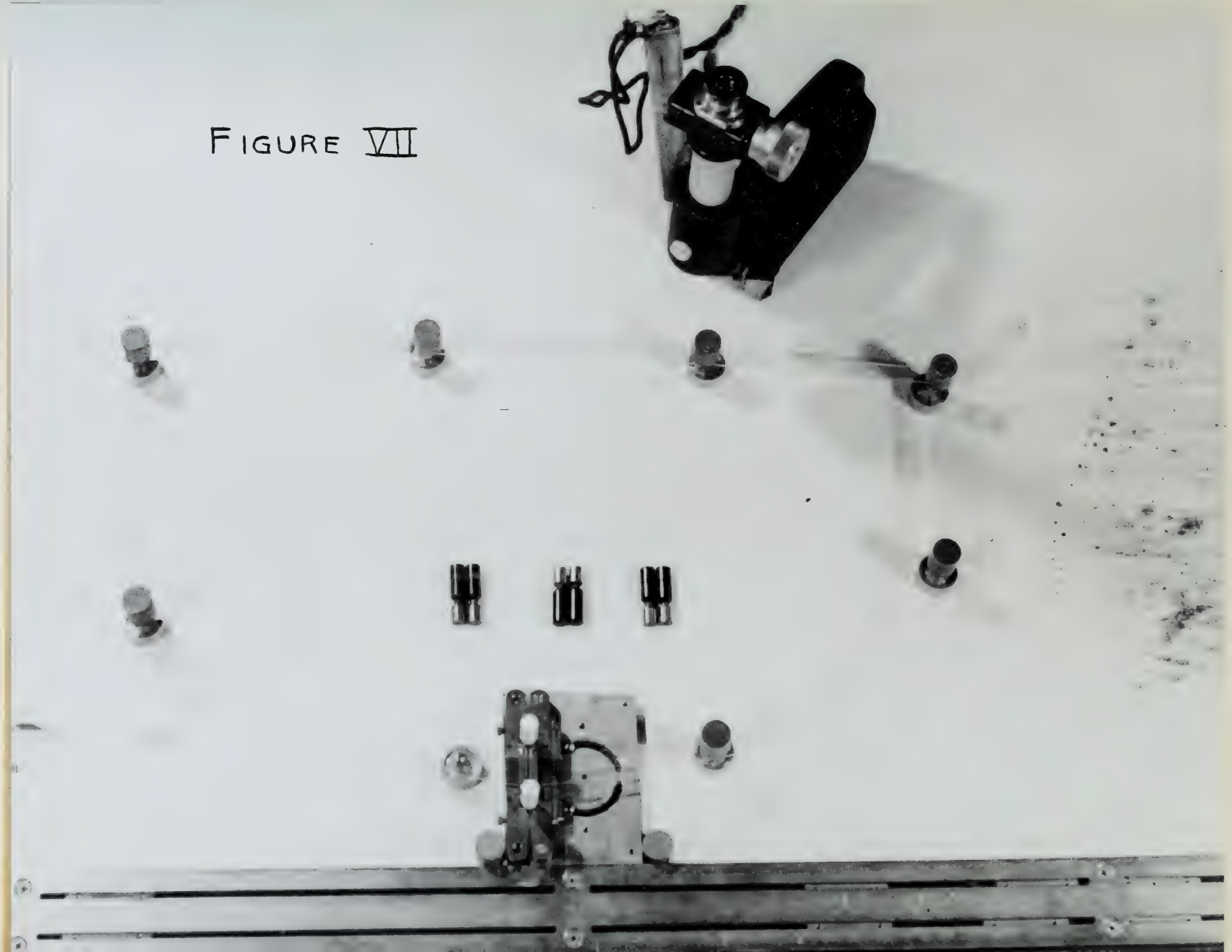

of a horizontal unit load as shown in Figure VIIIa. Betti's Law states that the external virtual work done by a system of forces, P, during the distortion caused by a system of forces, Q, is equal to the external virtual work done by the Q system during the distortion caused by the P system.

Figure VIII

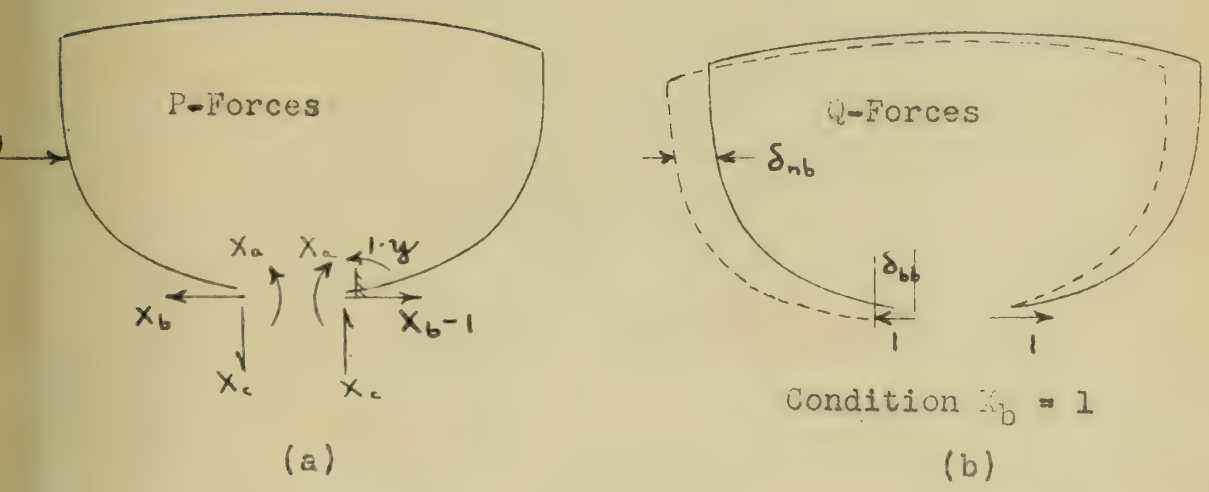

Applying Betti's Law to Figure VIII we can write:

$$\delta_b = 0 = 1 \cdot \delta_{nb} + X_b \delta_{bb} \qquad (1)$$

$$X_b = -\frac{\delta_{nb}}{\delta_{bb}}(1) \qquad (2)$$

Applying the Beggs method to equation (2) δ_{bb} is equal to the distortion introduced by one type of plug and δ_{nb} is the deflection measured at any point by the microscope.

In a similar manner expressions for X_a and X_c can be developed so that:

$$X_a = -\frac{na}{aa}(1) \qquad (3)$$

$$X_c = -\frac{nc}{cc}(1) \qquad (4)$$

Design of Model

The model used with the Beggs deformeter gage consisted of a planar celluloid representation of the characteristics of the original transverse frame. It was decided to make the model from a sheet of celluloid 1/16 in. thick and to the scale of 1/2 in. = 1 ft. 0 in. The characteristics of the prototype represented by the model were the shape of the neutral axis and the moment of inertia. These were obtained at 41 points spaced 16 in. apart along one-half the girth by reading the values from the curves represented by Figures IV and V in Appendix A. This large number of points was used to make the model closely approximate the actual variation in the moment of inertia. Similitude between the model and the prototype was attained by making the axial length k times that of the prototype and the moment of inertia of the model cross sections $\propto$ times those of the prototype. From this similitude, the ordinates to the influence lines for axial stress or shear on the model are equal to those on the prototype, but the ordinates of the influence line for any moment on the prototype are equal to 1/k times the corresponding ordinates on

the model. The scale of the model defines the proportionality factor k = 1/24. The proportionality constant, alpha (α), was assigned the value of 1/740,000. The selection of this constant determined the depth of the frame. This was limited to the 3/4" maximum that the Beggs deformeter gage can accommodate. The development of the formula for the determination of the depth of the model follows:

$$\alpha = \frac{I_m}{I_p} = 1/740,000 \qquad (5)$$

$$b = 1/16"$$

$$I_m = \frac{1}{12} bh^3 = \frac{h^3}{192} = \alpha I_p \qquad (6)$$

$$h = \sqrt[3]{192\ I_p} = \sqrt[3]{\frac{192 I_p}{740,000}} = 0.06375\ (I_p)^{1/3} \qquad (7)$$

The offsets, given in Table IV, for the curve of the neutral axis were determined by first drawing the molded line and then laying off the distances to the neutral axis.

Manufacture of Model

The model was manufactured by plotting the neutral axis on the sheet of celluloid. Half of the frame depth, as determined by equation (7), was laid off on each side of the neutral axis. The model was first sawed out and then filed to the proper depth. Table V gives a comparison of the actual depth of the model and the theoretical depth as determined by equation (7). Next the model was cut at the keel position and

Table IV

Table of Offsets and Moment of Inertia for Stations on Neutral Axis

Data from Large Scale Drawing

Stat. No.	Girth to Stat. on Mid Line ft.	I in^4	x ft.	y ft.
0	0		0	0
1	4.35	960	4.24	.62
2	8.65	805	8.42	1.48
3	13.00	464	12.50	2.37
4	17.40	400	16.12	4.90
5	21.83	353	17.54	8.42
6	26.28	344	19.66	12.54
7	30.50	372	20.01	16.30
8	35.00	263	20.05	21.11
9	40.13	253	19.40	21.53
10	45.17	253	10.04	21.84
11	50.04	253	5.02	21.99
12	55.25	253	0	22.05

Neutral Axis Girth-
¢ at base to dk. edge = 34'-3 3/8" = 34.281'
¢ at deck to dk. edge = 20'-1 1/2" = 20.125'

Station Spacing on Neutral Axis
0-6 - s = 4.215'
6-12 - s = 5.031'

Origin ¢ at Base Line

Table V
Model Depth

Station	I_p in^4	h in.	Port Actual Depth in.	Stbd. Actual Depth in.
0	1201	.678	.690*	.690*
1	995	.636	.639	.639
2	960	.629	.626	.628
3	960	.629	.625	.625
4	950	.627	.628	.625
5	911	.618	.626	.620
6	848	.603	.609	.604
7	749	.579	.572	.580
8	600	.537	.536	.544
9	497	.505	.502	.508
10	455	.490	.488	.495
11	431	.481	.478	.485
12	415	.476	.475	.476
13	401	.470	.468	.471
14	389	.465	.465	.466
15	376	.460	.461	.461
16	362	.455	.457	.451
17	351	.449	.447	.453
18	340	.445	.438	.447
19	340	.445	.436	.443
20	365	.456	.457	.459
21	384	.463	.459	.448
22	382	.463	.462	.449
23	371	.458	.454	.455
24	346	.448	.448	.440
25	299	.426	.428	.427
26	268	.411	--	--
27	253	.403	.404	.407
28	253	.403	.408	.403
29	253	.403	.406	.405
30	253	.403	.405	.405
31	253	.403	.405	.405
32	253	.403	.404	.403
33	253	.403	.404	.399
34	253	.403	.403	.399
35	253	.403	.404	.403
36	253	.403	.405	.401
37	253	.403	.405	.402
38	253	.403	.404	.405
39	253	.403	.402	.405
40	253	.403	.404	.401
41	253	.403	.404	.405
Top	253	.403		.404

* Not accurate--due to shape, micrometer cannot be used satisfactorily.

the ends rigidly clamped in the Beggs deformeter gage. The Beggs deformeter gage consists of two halves held together by springs. The right half of the gage was securely screwed to the table. With the deformeter gage are sets of plugs, which are inserted in the gage to make the two gage halves move relative to each other in rotation, horizontally or vertically. The plug sizes are such that one set causes relative rotation of 0.0104 radians, another set causes 0.0509" of relative horizontal displacement and the third set causes 0.0509" of relative vertical displacement of the ends. These distortions correspond to moment, thrust and shear, respectively.

The celluloid frame was supported at intervals by steel ball bearings resting on steel retainers. Weights were placed over the supports to make the frame stay flat. It was found that the weights produced frictional forces of sufficient magnitude to cause erratic results. To eliminate this, the weights were removed during the taking of data, and due care was used to be sure the frame remained flat.

Ordinates for the influence lines are to be determined for each of the 12 points along a half girth that were selected for use in the calculation of the influence lines. At these points, which were located on the model, microscope targets were glued.

A micrometer microscope was used to measure the deflections

which occurred at a point when each deformation was introduced by changing the plugs. Since the model was symmetrical, the redundants on the starboard side of the cut are either equal to those on the port side or differ from them by a statically determinate factor. This factor is equal to the support reaction corresponding to the redundant being considered. As a check on the measured deflections the starboard deflections were also measured. At a number of places, due probably to frictional effects, the redundants found from deflections of the port side were not consistent at all points. At these points the values used for the influence lines were the averages of the port and starboard deflections. The starboard readings used appear with the original data in Table XIX.

The deflections measured with the microscope are in microscope units. To apply the Müller-Breslau principle they must be in inches. The movement of a target on the plunger of an Ames dial indicator was measured in microscope units. This movement was compared with the movement registered in inches by the Ames dial. The calibration data are shown in Table XVIII, Appendix E. A calibration constant of .000186 inches per microscope unit was used throughout the experiment.

Evaluation of Influence Line Ordinates

Equations (2)-(4) and the similitude proportionality factor k form the basis for the calculation of the ordinates

of the influence lines.

$$X_a = -\frac{\delta_{na}}{\delta_{aa}} \times \frac{0.000186}{12\ k}\ (1)\ \frac{\text{micr.units}}{\text{radian}} \times \frac{\text{inches}}{\text{micr.unit}} \frac{\text{ft. kip}}{\text{inch}}$$

$$\delta_{aa} = 0.0104 \text{ radians}$$

$$X_b = -\frac{\delta_{nb}}{\delta_{bb}} \times 0.000186\ (1)\ \frac{\text{micr.units}}{\text{inches}} \times \frac{\text{inches}}{\text{micr.unit}} \times \text{kip}$$

$$\delta_{bb} = 0.0509 \text{ in.}$$

$$X_c = -\frac{\delta_{nc}}{\delta_{cc}} \times 0.000186\ (1)\ \frac{\text{micr.units}}{\text{inches}} \times \frac{\text{inches}}{\text{micr.unit}} \times \text{kip}$$

$$\delta_{cc} = 0.0509 \text{ in.}$$

In evaluating these expressions the average deflections for δ_{na}, δ_{nb}, and δ_{nc} given in Table XIX were used. The results are shown in Tables I and II.

APPENDIX C

Calculation of Influence Lines by the Elastic Center Method

The elastic center method consists of a special application of the law of virtual work, in which location of the redundants at the elastic center simplifies the solution of the equations. The method and the equations are derived in reference (4).

The effects of axial stress and shear are a small order of magnitude and were neglected. The positive direction of the redundants will be as shown in Figure IX. Applying the

Figure IX

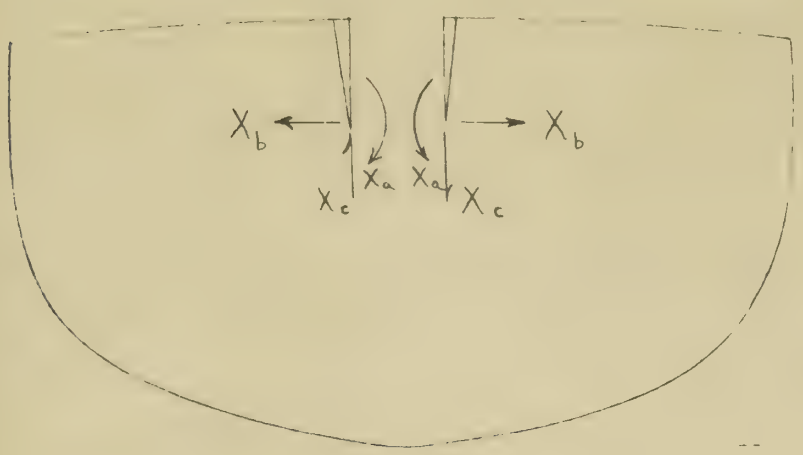

law of virtual work to this frame we can write the equations:

$$(1)\ \delta_a = 0 = \delta_{ao} + X_a\delta_{aa} + X_b\delta_{ab} + X_c\delta_{ac} \qquad (8)$$

$$(1)\ \delta_b = 0 = \delta_{bo} + X_a\delta_{ba} + X_b\delta_{bb} + X_c\delta_{bc} \qquad (9)$$

$$(1)\ \delta_c = 0 = \delta_{co} + X_a\delta_{ca} + X_b\delta_{cb} + X_c\delta_{cc} \qquad (10)$$

In the above equations δ refers to a deflection and X to a redundant force. The first subscript names the point whose deflection is under consideration at the moment and the direction of that deflection, while the second names the cause of the distortion. The subscript, o, indicates known external loadings.

By locating the redundants at the elastic center $\delta_{ab} = \delta_{ba} = \delta_{bc} = \delta_{cb} = \delta_{ac} = \delta_{ca} = 0$. Thus it is found that equations (8)-(10) simplify to

$$X_a = -\frac{\delta_{ao}}{\delta_{aa}} \qquad (11)$$

$$X_b = -\frac{\delta_{bo}}{\delta_{bb}} \qquad (12)$$

$$X_c = -\frac{\delta_{co}}{\delta_{cc}} \qquad (13)$$

The location of the elastic center was first determined by equation (14).

$$\bar{y} = \frac{\int y \frac{I_o}{I}\, ds}{\Sigma I_o A_e} \qquad (14)$$

$\bar{y}$ = distance from assumed axis to the elastic center

A_e = elastic weight

I_o was arbitrarily assumed = 960 in^4

Integration of equation (14) is shown in Table VI. Due to the symmetry of the frame, integration was carried halfway around and doubled. The elastic weight is equal to δ_{aa} and is evaluated by equation (15)

$$\delta_{aa} = \int M_a^2 \frac{ds}{EI} = \int 1^2 \frac{ds}{EI} = A_e \qquad (15)$$

$$EI_o\delta_{aa} = EI_oA_e = \frac{2 \times 4.285}{3} \times 2 \times 51.8612 = 296.3003$$

$$\bar{y} = \frac{\frac{2 \times 8}{3} \times 830.0717}{\frac{2 \times 8}{3} \times 51.8612} = 16.0056 \text{ ft.}$$

The origin was assumed at the molded base line on the centerline of the ship. The elastic center is located at y = 16.0056 ft. and, due to symmetry about the y axis, at x = 0. Let y_o be the vertical distance from a point to the elastic center. δ_{bb} was determined from equation (16). The integration of this equation is shown in Table I.

$$EI_o\delta_{bb} = \int M_b^2 \frac{I_o}{I} ds = \int y_o^2 \frac{I_o}{I} ds \qquad (16)$$

$$= 3121.1653 \times \frac{2 \times 4.285}{3} \times 2 = 17,832.2576$$

δ_{cc} was determined from equation (17). The integration of this equation is shown in Table VI.

$$EI_o\delta_{cc} = \int M_c^2 \frac{I_o}{I} ds = \int x_o^2 \frac{I_o}{I} ds \qquad (17)$$

$$= 10748.5039 \times \frac{4.285 \times 2}{3} \times 2 = 61409.7801$$

Table VI

Integration to Determine δ_{aa}, δ_{ab}, and δ_{bb}

Stat.	s	x ft.	y ft.	I_o/I	S.M.*	$s \cdot I_o/I \cdot$ Simp.Mult.	Simp.Mult. $\cdot y \cdot s \cdot I_o/I$	y_o	Simp.Mult. $\cdot y^2 \cdot s \cdot I_o/I$	Simp.Mult. $\cdot I_o/I \cdot x \cdot s$
0	1	0	.30	.7990	1/2	.3995	.1198	-13.1226	77.9417	--
1	1	4.24	1.00	1.0000	2	2.00	2.0000	-13.0356	430.3301	84.9552
2	1	8.48	1.60	1.1925	1	1.1925	2.7181	-14.1456	234.6169	95.7532
3	2	12.50	3.05	2.0690	2	4.1380	12.6416	-12.9556	694.5532	646.5525
4	1	16.12	5.40	2.3472	1	2.3472	12.3932	-10.7256	270.0184	669.9372
5	2	18.54	7.20	2.6116	2	5.3632	47.1962	- 7.2856	278.4609	1183.2113
6	1	19.66	14.12	.7907	1	.7907	36.0556	- 3.0456	26.5702	1077.6491
7	1	20.01	17.16	2.5066	2	5.1612	88.6494	+ 1.1344	7.2401	2066.3453
8	1	20.05	21.49	3.6502	1/2	1.8251	39.2214	+ 5.4844	54.0965	732.6447
8	1.174	20.05	21.49	3.6502	1/2	2.1427	46.0466	+ 5.4844	64.4495	861.3709
9	1.174	15.40	21.91	3.7945	2	8.9095	195.2071	+ 5.9144	311.6555	2112.1770
10	1.174	10.04	22.23	3.7945	1	4.4547	98.9844	+ 6.2344	177.5392	449.0409
11	1.174	5.02	22.37	3.7945	2	8.9095	199.3055	+ 6.3744	322.0195	224.5250
12	1.174	0	22.43	3.7945	1/2	4.4547	99.9603	+ 6.4344	177.2177	--
						51.8512	730.0717		3121.1053	10747.5730

* Simpson's Multipliers

In the stress analysis of this frame influence lines for the redundants caused by (1) a unit vertical load and (2) a unit horizontal load were determined. A stable and statically determinate structure that remains after the removal of the redundant forces is called a primary structure. Figure X shows the primary structure assumed.

Figure X

M_o is the bending moment in the primary structure caused by a unit load applied at a given point. For the primary structure

$$\delta_{ao} = \int M_a M_o \frac{I_o}{I} ds = \int M_o \frac{I_o}{I} ds \qquad (18)$$

$$\delta_{bo} = \int M_b M_o \frac{I_o}{I} ds = \int M_o y_o \frac{I_o}{I} ds \qquad (19)$$

$$\delta_{co} = \int M_c M_o \frac{I_o}{I} ds = \int M_o x \frac{I_o}{I} ds \qquad (20)$$

The integrations of δ_{ao}, δ_{bo}, and δ_{co} are shown in Table VII for a unit vertical load and in Table VIII for a unit horizontal load. The redundants are evaluated by equations (11)-(13). The numerical evaluation of these is shown in Table IX for a unit vertical load and in Table X for a unit horizontal load.

The values obtained for the redundants located at the elastic center are different from those obtained experimentally because of the difference in the location. Figure XI shows the two locations and the positive sense of the redundants. Equations (21)-(23) give the relationship between the redundants

Figure XI

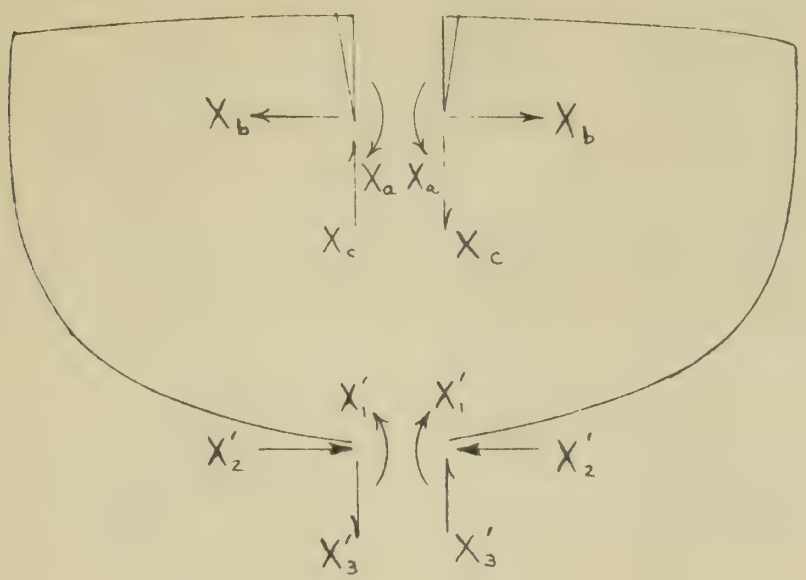

at the two locations when a vertical load is applied on the port side of the frame.

Table VII

Integration of δ_{ao}, δ_{bo}, δ_{co} for a Unit Load Applied Vertically

Load at Point 1p

Stat.	M_o	$M_o\frac{I}{I}$ds	$M_o\frac{I_o}{I}$yds	$M_o\frac{I_o}{I}$nds
0	- 4.24	- 1.6939 + 26.4078	0	
1	0	0	0	
2-12	0	0	0	0
Function		- 1.6939 + 26.4078	0	
Value		- 4.8369 + 75.4507	0	

Load at Point 2p

Stat.	M_o	$M_o\frac{I}{I}$ds	$M_o\frac{I_o}{I}$yds	$M_o\frac{I_o}{I}$nds
0	- 8.48	- 3.3878 + 52.9356	0	
1	- 4.24	- 8.4000 + 127.2475	+ 35.9552	
2-12	0	0	0	0
Function		- 11.8678 + 180.1831	+ 35.9552	
Value		- 33.9023 + 514.7230	+ 102.7120	

Load at Point 3p

Stat.	M_o	$M_o\frac{I}{I}$ds	$M_o\frac{I_o}{I}$yds	$M_o\frac{I_o}{I}$nds
0	-12.50	- 4.9938 + 78.0300	0	
1	- 8.26	- 10.5200 + 247.8925	+ 70.0448	
2	- 4.02	- 4.7939 + 67.8118	+ 40.6518	
3	0	0	0	0
4-12	0	0	0	0
Function		- 20.3077 + 393.7343	+ 110.0966	
Value		- 75.1523 +1124.7676	+ 316.2233	

Load at Point 4p

Stat.	M_o	$M_o\frac{I}{I}$ds	$M_o\frac{I_o}{I}$yds	$M_o\frac{I_o}{I}$nds
0	-16.12	- 6.4399 + 100.6275	0	
1	-11.88	- 23.7600 + 356.5331	+ 100.7424	
2	- 7.64	- 9.1107 + 128.8761	+ 77.2587	
3	- 3.62	- 14.9796 + 194.0693	+ 137.2445	
4-12	0	0	0	0
Function		- 54.2902 + 780.1060	+ 365.2456	
Value		-155.0690 +2228.6028	+1043.3849	

Load at Point 5p

Stat.	M_o	$M_o\frac{I}{I}$ds	$M_o\frac{I_o}{I}$yds	$M_o\frac{I_o}{I}$nds
0	-18.54	- 7.4067 + 115.7341	0	
1	-14.30	- 28.6000 + 429.1502	+ 121.2640	
2	-10.06	- 11.9960 + 169.3981	+ 101.7307	
3	- 6.04	- 24.9935 + 323.8062	+ 312.4190	
4	- 2.42	- 5.6802 + 80.9237	+ 91.5653	
5	0	0	0	0
6-12	0	0	0	0
Function		- 78.6770 +1099.3223	+ 626.9790	
Value		-424.7540 +3140.3973	+1791.0700	

Load at Point 6p

Stat.	M_o	$M_o\frac{I}{I}$ds	$M_o\frac{I_o}{I}$yds	$M_o\frac{I_o}{I}$nds
0	-19.66	- 7.8542 + 122.7256	0	
1	-15.42	- 30.8400 + 462.7727	+ 130.7616	
2	-11.18	- 13.3322 + 184.5909	+ 113.0566	
3	- 7.16	- 29.6281 + 383.8497	+ 370.3510	
4	- 3.54	- 8.3091 + 89.1199	+ 133.9426	
5	- 1.12	- 6.0068 + 43.2825	+ 111.3657	
6-12	0	0	0	0
Function		- 95.9704 +1289.6413	+ 859.4775	
Value		-274.1554 +3684.0752	+2455.2350	

Table VII (Continued)

Stat.	Load at Point 7p M_o	$M_o\frac{I_o}{I}ds$	$M_o\frac{I_o}{I}yds$	$M_o\frac{I_o}{I}xds$	Load at Point 8p M_o	$M_o\frac{I_o}{I}ds$	$M_o\frac{I_o}{I}yds$	$M_o\frac{I_o}{I}xds$
0	-20.01	- 7.9940	+124.9104	0	-20.05	- 8.0100	+125.1601	0
1	-15.77	-31.5400	+473.2766	+133.7296	-15.81	-31.6200	+474.4771	+134.0688
2	-11.53	-13.7495	+194.4950	+116.5960	-11.57	-13.7972	+195.1697	+117.0005
3	- 7.51	-31.0764	+402.6134	+388.4548	- 7.55	-31.2419	+404.7578	+390.5238
4	- 3.89	- 9.1306	+ 97.9311	+147.1855	- 4.93	-11.5717	+124.1132	+186.5359
5	- 1.47	- 7.8839	+ 56.8083	+146.1675	- 1.51	- 8.0984	+ 58.3541	+150.1449
6	- .35	- .9767	+ 3.0139	+ 19.2028	- .39	- 1.0884	+ 3.3583	+ 21.3974
7	0	0	0	0	- .04	- .2064	- .2445	+ 4.1310
8-12	0	0	0	0	0	0	0	0
Function		-102.3511	+1353.0487	+951.3362		-105.6340	+1365.1458	+1003.8023
Value		-292.3830	+3865.2090	+2717.6503		-301.7611	+3956.8997	+2867.5285

Stat.	Load at Point 9p M_o	$M_o\frac{I_o}{I}ds$	$M_o\frac{I_o}{I}yds$	$M_o\frac{I_o}{I}xds$	Load at Point 10p M_o	$M_o\frac{I_o}{I}ds$	$M_o\frac{I_o}{I}yds$	$M_o\frac{I_o}{I}xds$
0	-15.40	- 6.1523	+ 96.1330	0	-10.04	- 4.0110	+ 62.6737	0
1	-11.16	-22.3200	+334.9250	+ 94.6368	- 5.80	-11.6000	+174.0650	+ 49.1840
2	- 6.92	- 8.2521	+116.7307	+ 69.9778	- 1.56	- 1.8603	+ 26.3150	+ 15.7753
3	- 2.90	-12.0002	+155.4699	+150.0025	+ 2.46	+10.1795	-131.8813	-127.2435
4	+ .72	+ 1.6900	- 18.1261	- 27.2426	+ 6.08	+14.2710	-153.0646	-230.0484
5	+ 3.14	+16.8404	-121.3456	-312.2218	+ 8.50	+45.5872	-328.4834	-845.1865
6	+ 4.26	+11.8884	- 36.6829	-233.7258	+ 9.62	+26.8465	- 82.8378	-527.8032
7	+ 4.61	+23.7931	+ 28.1805	-476.1005	+ 9.97	+51.4572	+ 60.9456	-1029.6577
8	+ 4.65	+18.4503	+107.8233	-369.9280	+10.01	+39.7177	+232.1099	-796.3395
9	0	0	0	0	+ 5.36	+47.7549	+282.4414	-735.4258
10-12	0	0	0	0	0	0	0	0
Function		+23.9376	+663.1078	-1104.6016		+218.3427	+142.2835	-4220.7453
Value		+66.3817	+1894.2779	-3155.4785		+623.7323	+406.4565	-12074.4021

Table VII (Continued)

	Load at Point 11p				Load at Point 12p			
Stat.	M_o	$M_o\frac{I_o}{I}dx$	$M_o\frac{I_o}{I}ydx$	$M_o\frac{I_o}{I}xdx$	M_o	$M_o\frac{I_o}{I}dx$	$M_o\frac{I_o}{I}ydx$	$M_o\frac{I_o}{I}xdx$
0	- 5.02	- 2.0055	+ 31.3368	0	0	0	0	0
1	- .78	- 1.5600	+ 23.4087	+ 6.6144	+ 4.24	+ 8.48	-127.2475	- 35.9552
2	+ 3.46	+ 4.1261	- 53.3654	- 34.9889	+ 8.48	+ 10.1124	-143.0457	- 85.7532
3	+ 7.48	+30.9522	-401.0050	- 386.9030	+12.50	+ 51.7250	-670.1283	- 646.5625
4	+11.10	+26.0539	-279.4436	- 419.9896	+16.12	+ 37.8369	-405.8226	- 609.9308
5	+13.52	+72.5105	-522.6818	-1344.3436	+18.54	+ 99.4337	-716.4802	-1843.5008
6	+14.64	+40.8658	-126.0650	- 803.2265	+19.66	+ 54.8652	-169.2923	-1078.6498
7	+14.99	+77.3664	+ 91.6324	-1548.1012	+20.01	+103.2756	+122.3191	-2066.5448
8	+15.03	+59.6360	+348.5126	-1195.7026	+20.05	+ 79.5544	+464.9154	-1595.0657
9	+10.38	+92.4806	+546.9668	-1424.2014	+15.40	+137.2063	+811.4922	-2112.9770
10	+ 5.02	+22.3626	+139.1936	- 224.5205	+10.04	+ 44.7252	+278.3871	- 449.0410
11	0	0	0	0	+ 5.02	+ 44.7257	+285.0994	- 224.5230
12	0	0	0	0	0	0	0	0
Function Value		+422.7786	-206.3099	-7375.3629		+671.9404	-269.8039	-10748.5038
		+1207.7375	-589.3586	-21068.9529		+1919.5097	-770.7398	-30704.8918

Table VIII

Integration of δ_{ao}, δ_{bo}, δ_{co} for a Unit Load Applied Horizontally

Stat.	M_o	$M_o\frac{I_o}{I}ds$	$M_o\frac{I_o}{I}yds$	$M_o\frac{I_o}{I}xds$	M_o	$M_o\frac{I_o}{I}ds$	$M_o\frac{I_o}{I}yds$	$M_o\frac{I_o}{I}xds$
	Load at Point 1p					Load at Point 2p		
0	.62	+ .2477	- 3.8703	0	1.48	+ .5913	- 9.2338	0
1	0	0	0	0	.86	+ 1.7200	- 25.6096	- 7.2928
2-12	0	0	0	0	0	0	0	0
Function		+ .2477	- 3.8703	0		+ 2.3113	- 35.8434	- 7.2928
Value		+ .7076	- 11.0562	0		+ 6.6026	-100.1216	- 20.8331
	Load at Point 3p					Load at Point 4p		
0	2.67	+ 1.0667	- 16.6672	0	4.90	+ 1.9576	- 30.5678	0
1	2.05	+ 4.1000	- 61.5230	- 17.3840	4.28	+ 8.5600	-128.4479	- 36.2944
2	1.19	+ 1.4191	- 20.0736	- 12.0338	3.42	+ 4.0784	- 57.6906	- 34.5844
3	0	0	0	0	2.23	+ 9.2277	-119.5510	-115.3468
4-12	0	0	0	0	0	0	0	0
Function		+ 6.5858	- 98.2638	- 29.4178		+23.8237	-336.2773	-186.2256
Value		+18.8134	-280.7069	- 84.0368		+68.0564	-960.6321	-531.9845
	Load at Point 5p					Load at Point 6p		
0	8.42	+ 3.3638	- 52.5610	0	12.54	+ 5.0097	- 78.2797	0
1	7.80	+15.6000	-234.0874	- 66.1440	11.92	+23.8400	-357.7335	-101.0816
2	6.94	+ 8.2760	-117.0681	- 70.1801	11.06	+13.1891	-186.5667	-111.8431
3	5.75	+23.7935	-306.2592	-297.4188	9.87	+40.8421	-529.1337	-510.5256
4	3.52	+ 8.2621	- 88.6164	-133.1659	7.64	+18.0326	-192.3378	-289.0739
5	0	0	0	0	4.12	+22.0964	-159.2178	-409.6668
6-12	0	0	0	0	0	0	0	0
Function		+59.2944	-800.5921	-566.9288		+123.0099	-1503.2692	-1422.1912
Value		+169.3843	-2287.0247	-1619.5266		+351.3983	-4294.3389	-4062.7261

Table VIII (Continued)

Stat.	M_o	$M_o\frac{I_o}{I}ds$	$M_o\frac{I_o}{I}yds$	$M_o\frac{I_o}{I}xds$	M_o	$M_o\frac{I_o}{I}ds$	$M_o\frac{I_o}{I}yds$	$M_o\frac{I_o}{I}xds$
	Load at Point 7p				Load at Point 8p			
0	16.80	+ 6.7116	-104.8723	0	21.11	+ 8.4334	-131.7771	0
1	16.18	+32.3600	-485.5812	-137.2064	20.49	+40.9300	-614.9295	-173.7552
2	15.32	+18.2691	-258.4270	-154.9220	19.63	+23.4088	-331.1306	-198.5064
3	14.13	+52.4699	-757.5135	-730.8743	18.44	+76.3047	-968.5739	-953.8090
4	11.90	+27.9317	-299.5837	-450.2591	16.21	+38.0481	-408.0884	-613.3361
5	8.38	+44.9436	-323.8459	-833.2544	12.69	+68.0590	-490.4063	-1261.8137
6	4.26	+11.8884	- 36.6829	-233.7258	8.57	+23.9163	- 73.7963	-470.1948
7	0	0	0	0	4.31	+22.2448	+ 26.3466	-445.1178
8-12	0	0	0	0	0	0	0	0
Function		+200.5743	-2286.5065	-2540.2420		+301.3951	-3012.3555	-4116.5330
Value		+572.9732	-6474.6534	-7256.6245		+860.9853	-8605.2953	-11759.5623
	Load at Point 9p				Load at Point 10p			
0	21.53	+ 8.6012	-134.3989	0	21.84	+ 8.7251	-136.3340	0
1	20.91	+41.9800	-627.5342	-177.3168	21.22	+42.4400	-636.8377	-179.9456
2	20.05	+23.9096	-358.2154	-202.7536	20.36	+24.2793	-343.4447	-205.8885
3	18.86	+78.0427	-1011.0903	-975.5335	19.17	+79.3255	-1027.7095	-991.5683
4	16.63	+39.0339	-418.6619	-629.2276	16.94	+39.7616	-426.4662	-640.9571
5	13.11	+70.3116	-506.6373	-1303.5758	13.42	+71.9741	-518.6172	-1334.4003
6	8.99	+25.0884	- 77.4129	-493.2381	9.30	+25.9535	- 80.0823	-510.2464
7	4.73	+24.4125	+ 28.9140	-480.4936	5.04	+26.0124	+ 30.8090	-520.3090
8	.42	+ 1.6665	+ 9.7389	- 33.4128	.73	+ 2.8965	+ 16.9271	- 58.0747
9	0	0	0	0	.31	+ 2.7619	+ 16.3352	- 42.5340
10-12	0	0	0	0	0	0	0	0
Function		+313.0464	-3075.2980	-4303.5518		+324.1299	-3105.4203	-4484.1239
Value		+894.2692	-8785.1011	-12293.8127		+925.9311	-8871.1504	-12809.6470

Table VIII (Continued)

	Load at Point 11p				Load at Point 12p			
Stat.	M_o	$M_o\frac{I_o}{I}ds$	$M_o\frac{I_o}{I}yds$	$M_o\frac{I_o}{I}xds$	M_o	$M_o\frac{I_o}{I}ds$	$M_o\frac{I_o}{I}yds$	$M_o\frac{I_o}{I}xds$
0	21.99	+ 8.7850	-137.2704	0	22.05	+ 8.8090	-137.6449	0
1	21.37	+42.7400	-641.3393	-181.2176	21.43	+42.8600	-643.1400	-181.7264
2	20.51	+24.4582	-345.9750	-207.4053	20.57	+24.5297	-346.9871	-208.0121
3	19.32	+79.9462	-1035.7510	-999.3270	19.38	+80.1944	-1038.9676	-1002.4305
4	17.09	+40.1136	-430.2425	-646.6326	17.15	+40.2545	-431.7530	-648.9028
5	13.57	+72.7786	-524.4140	-1349.3153	13.63	+73.1004	-526.7327	-1355.2813
6	9.45	+26.3721	- 81.3740	-518.4761	9.51	+26.5396	- 81.8906	-521.7681
7	5.19	+26.7866	+ 31.7260	-536.0004	5.25	+27.0963	+ 32.0927	-542.1969
8	.88	+ 3.4917	+ 20.4053	- 70.0079	.94	+ 3.7297	+ 21.7965	- 74.7811
9	.46	+ 4.0984	+ 24.2394	- 63.1149	.52	+ 4.6329	+ 27.4010	- 71.3473
10	.15	+ .6682	+ 4.1592	- 6.7088	.21	+ .9355	+ 5.8228	- 9.3923
11	0	0	0	0	.06	+ .5346	+ 3.4076	- 2.6835
12	0	0	0	0	0	0	0	0
Function		+330.2386	-3115.8363	-4578.2059		+333.2166	-3116.5953	-4618.5223
Value		+943.3816	-8900.9055	-13078.4079		+951.8887	-8903.0737	-13193.5784

Table IX

Calculation of Redundants at Elastic Center due to Vertical Load

Stat.	$EI_o\delta_{ao}$ $M_o\frac{I_o}{I}ds$	X_a	$EI_o\delta_{bo}$ $M_o\frac{I_o}{I}yds$	X_b	$EI_o\delta_{co}$ $M_o\frac{I_o}{I}xds$	X_c
0	0	0	0	0	0	0
1	- 4.8389	+ .0163	+ 75.6097	-.00424	0	0
2	- 33.9023	+ .1144	+ 514.7230	-.02886	+ 102.7120	.001673
3	- 75.1523	+ .2536	+1124.7676	-.06307	+ 316.2233	.005149
4	- 155.0890	+ .5234	+2228.5028	-.1250	+ 1043.3849	.01699
5	- 224.7540	+ .7585	+3140.3973	-.1761	+ 1791.0700	.02917
6	- 274.1554	+ .9253	+3684.0752	-.2066	+ 2455.2350	.03998
7	- 292.3830	+ .9868	+3865.2090	-.2167	+ 2717.6503	.04425
8	- 301.7611	+1.0184	+3956.8997	-.2219	+ 2867.5285	.04669
9	+ 68.3817	- .2308	+1894.2779	-.1062	- 3155.4785	.05138
10	+ 623.7323	-2.1051	+ 406.4565	-.0228	-12074.4021	.1966
11	+1207.7375	-4.0761	- 589.3586	+.0331	-21068.9529	.3431
12	+1919.5097	-6.4783	- 770.7398	+.04322	-30704.8918	.5000
	$EI_o\delta_{aa}$ = 296.3003		$EI_o\delta_{bb}$ = 17832.2576		$EI_o\delta_{cc}$ = 61409.7801	

Table X

Calculation of Redundants at Elastic Center due to Horizontal Load

Stat.	$EI_o\delta_{ao} = \int_o \frac{I_o}{I} x_o ds$	X_a	$EI_o\delta_{bo} = \int_o \frac{I_o}{I} y_o ds$	X_b	$EI_o\delta_{co} = \int_o \frac{I_o}{I} \alpha_o ds$	X_c
0	0	0	0	0	0	0
1	+ .7076	- .002388	- 11.0562	+.00062	0	0
2	+ 6.6026	- .02228	-100.1216	+.005615	- 20.6731	+.00339
3	+ 18.8134	- .06349	-280.7069	+.01574	- 84.0363	+.01368
4	+ 68.0564	- .2297	-960.6321	+.05387	- 331.[illegible]45	+.05863
5	+169.3043	- .5717	-2237.0247	+.1263	- 1619.5266	+.02637
6	+351.3983	-1.1860	-4294.3389	+.2408	- 4062.7261	+.06616
7	+572.9739	-1.9338	-6474.6534	+.3631	- 7256.6245	+.1182
8	+860.9563	-2.9038	-8605.2953	+.4826	-11759.5623	+.1915
9	+994.2692	-3.0181	-8765.1011	+.4917	-12291.8127	+.2002
10	+925.9311	-3.1250	-8971.1504	+.4975	-12809.8470	+.2086
11	+943.3816	-3.1839	-8900.9055	+.4991	-13074.4079	+.2130
12	+951.3077	-3.2126	-8903.0737	+.4993	-13193.5734	+.2148
	$EI_o\delta_{aa}$ = 296.3003		$EI_o\delta_{bb}$ = 1783.2976		$EI_o\delta_{cc}$ = 61409.7801	

$$X'_1 = X_a - y_o X_b - x \cdot 1 \qquad (21)$$

$$X'_2 = X_b \qquad (22)$$

$$X'_3 = X_c - 1 \qquad (23)$$

Equations (24)-(26) give the relationship between the redundants at the two locations when a horizontal load is applied on the port side of the frame.

$$X'_1 = X_a - y_o X_b + y \cdot 1 \qquad (24)$$

$$X'_2 = X_b - 1 \qquad (25)$$

$$X'_3 = X_c \qquad (26)$$

The evaluation of equations (21) and (23)-(25) is shown in Table XI for a unit vertical load and in Table XII for a unit horizontal load.

Table XI

Transfer of Redundants to Relocate at Station 0
Due to Unit Vertical Load

Stat.	X_a	$y_o X_b$	$X_a - y_o X_b$	x	X_1' $(X_a - y_o X_b - x)$	X_c	X_3' $(X_c - 1)$
0							
1	+ .0163	- .0663	+ .0826	4.24	- 4.1574	0	-1.0000
2	+ .1144	- .4510	+ .5654	8.48	- 7.9146	-.001673	-1.001673
3	+ .2536	- .9855	+1.2391	12.50	-11.2609	-.005149	-1.005149
4	+ .5234	-1.9527	+2.4761	16.12	-13.6439	-.0170	-1.0170
5	+ .7585	-2.7668	+3.5253	18.54	-15.0147	-.0292	-1.0292
6	+ .9253	-3.2282	+4.1535	19.66	-15.5065	-.0400	-1.0400
7	+ .9868	-3.3868	+4.3736	20.01	-15.6364	-.0443	-1.0443
8	+1.0184	-3.4673	+4.4857	20.05	-15.5643	-.0467	-1.0467
9	- .2308	-1.6599	+1.4291	15.40	-13.9709	+.0513	- .9486
10	-2.1051	- .3561	-1.7490	10.04	-11.7890	+.1966	- .8034
11	-4.0761	+ .5164	-4.5925	5.02	- 9.6125	+.3431	- .6569
12	-6.4783	+ .6753	-7.1536	0	- 7.1536	+.5000	- .5000

Table XII

Transfer of Redundants to Relocate at Station 0
Due to Unit Horizontal Load

Stat.	X_a	$y_o\bar{X}_b$	$X_a - y_o\bar{X}_b$	y	$X_1' (X_a - y_o\bar{X}_b + y)$	$\bar{X}_b$	$X_2' (\bar{X}_b - 1)$
0							
1	- .002318	+ .009689	- .012077	.62	+ .6079	+.00062	-.99938
2	- .022283	+ .087738	- .110021	1.48	+ 1.370	+.005615	-.994385
3	- .063494	+ .245978	- .309472	2.67	+ 2.3605	+.01574	-.98425
4	- .229687	+ .841751	- 1.071438	4.90	+ 3.8286	+.05387	-.94613
5	- .571664	+2.004014	- 2.575678	8.42	+ 5.8443	+.1283	-.8717
6	-1.186000	+3.762941	- 4.948941	12.54	+ 7.5911	+.2409	-.7591
7	-1.933761	+5.673452	- 7.607213	16.80	+ 9.1928	+.3631	-.6369
8	-2.905786	+7.540430	-10.446216	21.11	+10.6636	+.4826	-.5174
9	-3.018118	+7.697983	-10.716101	21.53	+10.8139	+.4926	-.5073
10	-3.124975	+7.773392	-10.898367	21.84	+10.9416	+.4975	-.5025
11	-3.183870	+7.799456	-10.983326	21.99	+11.0067	+.4991	-.5008
12	-3.212581	+7.801362	-11.013943	22.05	+11.0361	+.4993	-.5007

APPENDIX D

Calculation of Influence Lines for the Redundants by the Hovgaard Method

The general mathematical treatment and applications of the formulae are described by Dr. Willian Hovgaard in reference (5).

Briefly, the procedure followed was to apply a unit vertical load at one station and solve for the redundants. This was repeated for every station; then the whole procedure was repeated for a unit horisontal load. The results were plotted as a family of influence lines.

The following assumptions were made:

(1) The neutral axis of the ship frame forms a continuous closed curve, interrupted by a point of sharp curvature at the deck edge.

(2) The intersection of the neutral axis with the centerline just above the keel was used as the origin of coordinate axes, and was the place at which the bending moment, thrust and shear were found.

(3) Only the deformation caused by bending was considered; deformations caused by axial and shear forces were neglected.

The equations fundamental to the Hovgaard method are:

$$\int_0^0 \frac{M}{I}\, ds = 0 \qquad (27)$$

$$\int_o^o y \frac{M}{I} ds = 0 \qquad (28)$$

$$\int_o^o x \frac{M}{I} ds = 0 \qquad (29)$$

where:

M = bending moment at a point due to all forces

x = horizontal coordinate of a point

y = vertical coordinate of a point

I = moment of inertia

Inch units are used for moment of inertia; kip and feet units were used for other terms.

The value of M depends on the loading system and the nature of the redundants. In Figure XII the redundants are

Figure XII

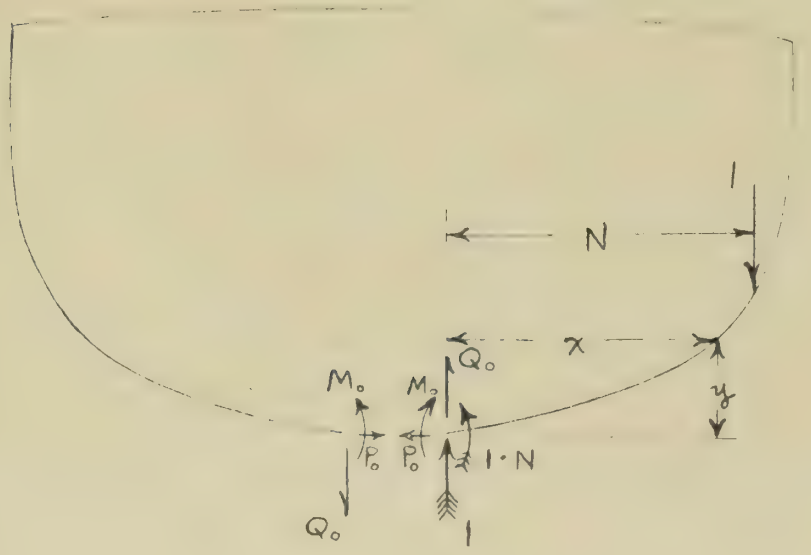

shown in their positive sense. A unit vertical load was

applied and an additional force and couple were inserted at station 0 in order to maintain equilibrium. The support reactions vanish when actual use is made of the influence lines. The moment at any station (A) is

$$M = M_o + P_o y + Q_o x + 1 \cdot x - 1 \cdot N$$

$$= M_o + P_o y + Q_o x \mp N + x \qquad (30)$$

Integration was done halfway around the frame and advantage taken of symmetry. Simpson's rule was used for integration with eight stations selected between the keel and the deck edge, and four more stations selected between the deck edge and the center of the deck. The spacing of stations 0 to 8 was 4.285 feet and of stations 8 to 12 was 5.031 feet. All terms were divided through by 4.285, yielding "station factors" of 1 and 1.174, which were easier to tabulate.

Use was made of Professor G. G. Manning's method of organizing the work in the following equations.

Substituting M in equation (27)

$$\int \frac{M}{I}\,ds = \int \frac{ds}{I}\,(M_o + P_o y + Q_o x \mp N + x) = 0 \qquad (31)$$

Integrating term by term with Simpson's rule we have

$$\int \frac{M_o}{I}\,ds = M_o \frac{2\delta}{3}\left(\frac{1}{2I_o} + \frac{2}{I_1} + \frac{1}{I_2} + \frac{2}{I_3} + \cdots \frac{1}{2I_{12}}\right) = \frac{2\delta}{3}\,\alpha\,M_o \qquad (32)$$

$$\int \frac{P_o y}{I}\,ds = P_o \frac{2\delta}{3}\left(\frac{y_o}{2I_o} + \frac{2y_1}{I_1} + \frac{y_2}{I_2} + \frac{2y_3}{I_3} + \cdots \frac{y_{12}}{2I_{12}}\right) = \frac{2\delta}{3}\,\beta\,P_o \qquad (33)$$

$$\int \frac{x}{I}ds = \frac{2s}{3}\left(\frac{x_0}{2I_0} + \frac{2x_1}{I_1} + \frac{x_2}{I_2} + \frac{2x_3}{I_3} + \ldots + \frac{x_{12}}{2I_{12}}\right) - \frac{2s}{3}\gamma_{x_0} \quad (34)$$

$$\int \frac{(x-H)}{I}ds = \frac{2s}{3}\left(\frac{x_0-H}{2I_0} + \frac{2(x_1-H)}{I_1} + \frac{x_2-H}{I_2} + \frac{2(x_3-H)}{I_3} + \ldots + \frac{x_{12}-H}{2I_{12}}\right) = \frac{2s}{3}\varepsilon \quad (35)$$

Substitute (32) (33) (34) and (35) in equation (31), divide through by $\frac{2s}{3}$ and the result is

$$\alpha H_o + \beta P_o + \gamma Q_o + \varepsilon = 0 \quad (36)$$

Similarly, from equations (28) and (29), one may derive:

$$\alpha_1 H_o + \beta_1 P_o + \gamma_1 Q_o + \varepsilon_1 = 0 \quad (37)$$

$$\alpha_2 H_o + \beta_2 P_o + \gamma_2 Q_o + \varepsilon_2 = 0 \quad (38)$$

The values of ε, ε_1 and ε_2 depend on the external loading system.

The values of α, β and γ are constant. In Table XIII are found the values of $\frac{\alpha}{2}$, $\frac{\beta}{2}$, and $\frac{\gamma}{2}$. Doubling gives:

α = .108020	β = 1.688090	γ = 0
α_1 = 1.688090	β_1 = 32.872740	γ_1 = 0
α_2 = 0	β_2 = 0	γ_2 = 22.388912

The values of ε, ε_1 and ε_2 were found, for the vertical load, by the integrations shown in Table XIV.

The simultaneous equations (36), (37) and (38) were solved in Tables XVI and XVII.

Table XIII

Hovgaard Method

Calculation of Coefficients of H_o, P_o, and Q_o

Stat.	(1) x ft.	(2) y ft.	(3) Mult.*	(4) Stat. Dist.	(5) (3)x(4)	(6) I_c in^4	(7) (5)÷(6)	(8) y x(7)	(9) x x(7)	(10) y x(8)	(11) x x(8)	(12) x x(9)
0	0	0	1/2	1	1/2	1201	.0004163	0	0	0	0	0
1	4.24	.62	2	1	2	960	.002080	.001290	.008819	.[illegible]	.005470	.037393
2	8.48	1.48	1	1	1	805	.001240	.001835	.010515	.002716	.015561	.089167
3	12.50	2.67	2	1	2	464	.004310	.011508	.053875	.030726	.143850	.673436
4	16.12	4.90	1	1	1	409	.002440	.011956	.039333	.058584	.192731	.634040
5	18.54	8.42	2	1	2	358	.005586	.047034	.103564	.396026	.872011	1.920077
6	19.66	12.54	1	1	1	344	.002907	.036454	.057152	.457133	.716668	1.123608
7	20.01	16.80	2	1	2	372	.005376	.090317	.107574	1.517326	1.807243	2.152556
8	20.05	21.11	1/2	2.174	1.087	263	.004133	.087246	.052067	1.841805	1.749322	1.661483
9	15.40	21.53	2	1.174	2.348	253	.009281	.199820	.142927	4.302125	3.077228	2.201076
10	10.04	21.84	1	1.174	1.174	253	.004640	.101338	.046586	2.213222	1.017434	.467723
11	5.02	21.99	2	1.174	2.348	253	.009281	.204089	.046591	4.487917	1.024527	.233887
12	0	22.05	1/2	1.174	.587	253	.002320	.051156	0	1.127990	0	0
							.054010	.944045	.699803	18.436370	10.622063	11.194456

*Simpson's Multiplier

Table IV

Calculation of ε, ε_1, and ε_2 due to Unit Vertical Load

Stat.	(13)	(14)	ε (7)x(14)	ε_1 (8)x(14)	ε_2 (9)x(14)	(13)	(14)	ε (7)x(14)	ε_1 (8)x(14)	ε_2 (9)x(14)
	Load at Station 1s							Load at Station 2s		
0	4.24	- 4.24	-.001765	0	0	8.48	- 8.48	-.003530	0	0
1	4.24	0	0	0	0	8.48	- 4.24	-.003530	-.005470	-.037393
2-12	4.24	0	0	0	0	8.48	0	0	0	0
			-.001765	0	0			-.007060	-.005470	-.037393
	Load at Station 3s							Load at Station 4s		
0	12.50	-12.50	-.005204	0	0	16.12	-16.12	-.006711	0	0
1	12.50	- 8.26	-.017181	-.010655	-.072845	16.12	-11.88	-.024710	-.015325	-.104770
2	12.50	- 4.02	-.004985	-.007377	-.042270	16.12	- 7.64	-.009474	-.014019	-.080335
3	12.50	0	0	0	0	16.12	- 3.62	-.015002	-.041859	-.195028
4-12	12.50	0	0	0	0	16.12	0	0	0	0
			-.027370	-.018032	-.115115			-.056497	-.071003	-.380133
	Load at Station 5s							Load at Station 6s		
0	16.54	-16.54	-.007718	0	0	19.66	-19.66	-.009184	0	0
1	16.54	-14.30	-.029744	-.018447	-.126112	19.66	-15.42	-.032074	-.019892	-.135989
2	16.54	-10.06	-.012474	-.018460	-.102701	19.66	-11.18	-.013863	-.020515	-.114155
3	16.54	- 6.04	-.026032	-.069508	-.325405	19.66	- 7.16	-.030860	-.082397	-.385745
4	16.54	- 2.42	-.005905	-.015934	-.095186	19.66	- 3.54	-.008638	-.042324	-.252936
5	16.54	0	0	0	0	19.66	- 1.12	-.006256	-.052678	-.115992
6-12	16.54	0	0	0	0	19.66	0	0	0	0
			-.081873	-.13.349	-.652434			-.0[illegible]75	-.217[illegible]36	-.[illegible]4573

Table XIV (Continued)

Stat.	(13) X	(14) x-X	ε_7 (7)x(14)	ε_8 (8)x(14)	ε_9 (9)x(14)	(13) X	(14) x-X	ε_7 (7)x(14)	ε_8 (8)x(14)	ε_9 (9)x(14)
			Load at Station 7s					Load at Station 8s		
0	20.01	-20.01	-.006330	0	0	20.05	-20.05	-.006347	0	0
1	20.01	-15.77	-.032802	-.020343	- .139076	20.05	-15.81	-.032869	-.020395	- .139428
2	20.01	-11.53	-.014297	-.021158	- .121238	20.05	-11.57	-.014347	-.021231	- .121659
3	20.01	- 7.51	-.032368	-.000425	- .404601	20.05	- 7.55	-.032541	-.000685	- .406756
4	20.01	- 3.89	-.009492	-.046509	- .153005	20.05	- 4.93	-.012029	-.058943	- .193912
5	20.01	- 1.47	-.008211	-.069140	- .152239	20.05	- 1.51	-.008435	-.071021	- .156352
6	20.01	- .35	-.001017	-.012759	- .020003	20.05	- .39	-.001134	-.014217	- .022289
7	20.01	0	0	0	0	20.05	- .04	-.000215	-.003613	- .004303
8-12	20.01	0	0	0	0	20.05	0	0	0	0
			-.100517	-.256334	- .990162			-.100933	-.276305	-1.044729
			Load at Station 9s					Load at Station 10s		
0	15.40	-15.40	-.006411	0	0	10.04	-10.04	-.004180	0	0
1	15.40	-11.16	-.023213	-.014396	- .093420	10.04	- 5.80	-.012064	-.007482	- .048550
2	15.40	- 6.92	-.008581	-.012696	- .072764	10.04	- 1.56	-.001934	-.002863	- .016403
3	15.40	- 2.90	-.012499	-.033373	- .156230	10.04	+ 2.46	+.010603	+.028310	+ .132533
4	15.40	+ .72	+.001757	+.004600	+ .021320	10.04	+ 6.68	+.016035	+.042692	+ .197845
5	15.40	+ 3.14	+.017540	+.147687	+ .325191	10.04	+ 8.50	+.047481	+.399739	+ .880294
6	15.40	+ 4.26	+.018334	+.155294	+ .243468	10.04	+ 9.62	+.027765	+.350687	+ .549802
7	15.40	+ 4.61	+.024783	+.416361	+ .495916	10.04	+ 9.97	+.053599	+.900460	+1.072513
8	15.40	+ 4.65	+.019218	+.405703	+ .305332	10.04	+10.01	+.041371	+.873352	+ .662499
9	15.40	0	0	0	0	10.04	+ 5.36	+.049746	+1.071035	+ .766039
10-12	15.40	0	0	0	0	10.04	0	0	0	0
			+.024776	+1.079100	+1.[illegible]			+.277422	+3.[illegible]	+4.402322

Table XIV (Continued)

Stat.	(13) N	(14) x-N	ε (7)x(14)	ε_1 (8)x(14)	ε_2 (9)x(14)	(13) N	(14) x-N	ε (7)x(14)	ε_1 (8)x(14)	ε_2 (9)x(14)
	Load at Station 11s						Load at Station 12s			
0	5.02	- 5.02	-.002090	0	0	0	0	0	0	0
1	5.02	- .78	-.000162	-.000106	- .006879	0	+ 4.24	+.000819	+.005470	+ .037393
2	5.02	+ 3.46	+.004290	+.006349	+ .036382	0	+ 8.48	+.010915	+.015561	+ .089167
3	5.02	+ 7.48	+.032239	+.046080	+ .402985	0	+12.50	+.053875	+.113850	+ .973438
4	5.02	+11.10	+.027084	+.132712	+ .436596	0	+16.12	+.039333	+.192731	+ .634048
5	5.02	+13.52	+.075523	+.635900	+1.400135	0	+18.54	+.103564	+.872010	+1.920077
6	5.02	+14.64	+.042558	+.533687	+ .836705	0	+19.66	+.057152	+.716636	+1.123608
7	5.02	+14.99	+.080586	+1.353852	+1.612534	0	+20.01	+.107574	+1.807243	+2.152556
8	5.02	+15.03	+.062119	+1.311337	+1.245491	0	+20.05	+.082867	+1.749322	+1.661483
9	5.02	+10.38	+.096337	+2.074132	+1.483582	0	+15.40	+.142927	+3.077228	+2.201076
10	5.02	+ 5.02	+.023293	+.508717	+ .233862	0	+10.04	+.046586	+1.017434	+ .467723
11	0	0	0	0	0	0	+ 5.02	+.046591	+1.024527	+ .233887
12	0	0	0	0	0	0	0	0	0	0
			+.440317	+6.41760	+7.001443			+.[illegible]	+[illegible]	+[illegible]

Table IV
Hovgaard Method
Calculation of ε, ε_1, and ε_2 due to Unit Horizontal Load

Stat.	(13) H	(14) y-H	ε (7)x(14)	ε_1 (8)x(14)	ε_2 (9)x(14)	(13) H	(14) y-H	ε (7)x(14)	ε_1 (8)x(14)	ε_2 (9)x(14)
			Load at Station 1s					Load at Station 2s		
0		- .62	+.000258	0	0	1.48	- 1.43	+.000616	0	0
1	.62	0	0	0	0	1.48	- .86	+.001789	+.001109	+.007584
2-12	.62	0	0	0	0	1.48	0	0	0	0
			+.000258					+.002405	+.001109	+.007584
			Load at Station 3s					Load at Station 4s		
0	2.67	- 2.67	+.001112	0	0	4.90	- 4.90	+.002040	0	0
1	2.67	- 2.05	+.004264	+.002645	+.018079	4.90	- 4.28	+.008902	+.005521	+.037745
2	2.67	- 1.19	+.001476	+.002184	+.012513	4.90	- 3.42	+.004241	+.006276	+.035961
3	2.67	0	0	0	0	4.90	- 2.23	+.009611	+.025663	+.120141
4-12	2.67	0	0	0	0	4.90	0	0	0	0
			+.006852	+.004829	+.030592			+.024794	+.037460	+.193847
			Load at Station 5s					Load at Station 6s		
0	8.42	- 8.42	+.003505	0	0	12.54	-12.54	+.005220	0	0
1	8.42	- 7.80	+.016224	+.010062	+.064788	12.54	-11.92	+.024794	+.015377	+.105122
2	8.42	- 6.94	+.011606	+.012735	+.072974	12.54	-11.06	+.013714	+.020295	+.116296
3	8.42	- 5.75	+.023783	+.066171	+.306731	12.54	- 9.87	+.042540	+.113584	+.531746
4	8.42	- 3.52	+.006569	+.042805	+.139452	12.54	- 7.64	+.010642	+.091344	+.300504
5	8.42	0	0	0	0	12.54	- 4.12	+.023014	+.193780	+.426684
6-12	8.42	0	0	0	0	12.54	0	0	0	0
			+.060707	+.131053	+.583925			+.127924	+.434380	+.4 0352

Table XI (Continued)

Sta.	(13) I	(14) y-Ī	ε (7)x(14)	ε_1 (8)x(14)	ε_2 (9)x(14)	(13) II	(14) y-Ī	ε (7)x(14)	ε_1 (8)x(14)	ε_2 (9)x(14)
	Load at Station 7s'					Load at Station 8s				
0	16.80	-16.80	+.006994	0	0	21.11	-21.11	+.008788	0	0
1	16.80	-16.18	+.033654	+.020713	+.142691	21.11	-20.49	+.042619	+.026432	+.182701
2	16.80	-15.32	+.018977	+.026112	+.161090	21.11	-19.63	+.024341	+.036021	+.206409
3	16.80	-14.13	+.060900	+.162608	+.761294	21.11	-18.44	+.079476	+.212208	+.993455
4	16.80	-11.90	+.029036	+.142276	+.460063	21.11	-16.21	+.039552	+.193707	+.637224
5	16.80	- 8.38	+.046811	+.394145	+.807866	21.11	-12.69	+.070886	+.596661	+1.314227
6	16.80	- 4.26	+.012384	+.155204	+.243468	21.11	- 8.57	+.024913	+.312411	+.490793
7	16.80	0	0	0	0	21.11	- 4.31	+.023171	+.309266	+.463614
8-12	16.80	0	0	0	0	21.11	0	0	0	0
			+.208770	+.903957	+2.024432			+.313746	+2.707006	+4.295617
	Load at Station 9s					Load at Station 10s				
0	21.53	-21.53	+.009963	0	0	21.84	-21.84	+.009092	0	0
1	21.53	-20.91	+.043493	+.026974	+.184405	21.84	-21.22	+.044138	+.027374	+.187139
2	21.53	-20.05	+.024662	+.036792	+.210826	21.84	-20.36	+.025246	+.037361	+.214065
3	21.53	-18.86	+.061287	+.217041	+1.016063	21.84	-19.17	+.063623	+.220608	+1.032764
4	21.53	-16.63	+.040577	+.198824	+.694108	21.84	-16.94	+.041334	+.202535	+.666301
5	21.53	-13.11	+.073232	+.610616	+1.357724	21.84	-13.42	+.074964	+.631197	+1.389829
6	21.53	- 8.99	+.026134	+.327721	+.513796	21.84	- 9.30	+.027035	+.339022	+.531514
7	21.53	- 4.73	+.025420	+.427199	+.508825	21.84	- 5.04	+.027095	+.455190	+.542173
8	21.53	- 0.42	+.001736	+.036644	+.034864	21.84	- 0.73	+.003017	+.063691	+.060493
9	21.53	0	0	0	0	21.84	- 0.31	+.002877	+.061944	+.044307
10-12	21.53	0	0	0	0	21.84	0	0	0	0
			+.324723	+2.927119	+5.431571			+.337421	+2.971030	+5.663625

Table XV (Continued)

Sta.	(13) H	(14) y-H	ε (7)x(14)	ε1 (8)x(14)	ε2 (9)x(14)	(13) H	(14) y-H	ε (7)x(14)	ε1 (8)x(14)	ε2 (9)x(14)
	Load at Station 11s					Load at Station 12s				
0	21.99	-21.99	+.009154	0	0	22.05	-22.05	+.009179	0	0
1	21.99	-21.37	+.044459	+.027567	+.188462	22.05	-21.43	+.044574	+.027645	+.188991
2	21.99	-20.51	+.025432	+.037636	+.215663	22.05	-20.57	+.025507	+.037746	+.216294
3	21.99	-19.32	+.063269	+.232335	+1.040365	22.05	-19.38	+.063520	+.233225	+1.044090
4	21.99	-17.99	+.041700	+.204328	+.672701	22.05	-17.15	+.041846	+.205045	+.674561
5	21.99	-13.57	+.075092	+.638291	+1.405353	22.05	-13.63	+.076137	+.641073	+1.411577
6	21.99	- 9.45	+.027471	+.344490	+.540086	22.05	- 9.51	+.027640	+.346671	+.543516
7	21.99	- 5.19	+.027901	+.463745	+.556309	22.05	- 5.25	+.028224	+.474164	+.564764
8	21.99	- 0.82	+.003637	+.076772	+.072923	22.05	- 0.94	+.003885	+.082013	+.077895
9	21.99	- 0.46	+.004269	+.091017	+.085746	22.05	- 0.52	+.004826	+.103906	+.097832
10	21.99	- 0.15	+.000696	+.015201	+.006963	22.05	- 0.21	+.000974	+.021281	+.009753
11	21.99	0	0	0	0	22.05	- 0.06	+.000357	+.012245	+.002795
12	21.99	0	0	0	0	22.05	0	0	0	0
			+.343761	+2.127243	+4.706606			+.346603	+2.171171	+4.728196

Table XVI

Hovgaard Method--Vertical Unit Load
Solution of Simultaneous Equations

Load at Stat.	Coef. of M_o +	Coef. of P_o =	$-.0513528\varepsilon_1$	M_o	$1 \cdot \Pi$	$M+M_o$
	.100020	1.688090	+.001765			
	-.078687	1.688090	0			
1	.021333	0	+.001765	+ .0827	- 4.24	- 4.1573
			+.012349			
			+.000281			
2	"	"	+.012068	+ .5657	- 8.48	- 7.9143
			+.027370			
			+.000926			
3	"	"	+.026444	+1.2396	-12.50	-11.2604
			+.056497			
			+.003646			
4	"	"	+.052851	+2.4774	-16.12	-13.6426
			+.081873			
			+.006950			
5	"	"	+.074923	+3.5121	-18.54	-15.0279
			+.099875			
			+.011185			
6	"	"	+.088690	+4.1574	-19.66	-15.5026
			+.106517			
			+.013163			
7	"	"	+.093354	+4.3760	-20.01	-15.6340
			+.109933			
			+.014189			
8	"	"	+.095744	+4.4881	-20.05	-15.5619
			-.024978			
			-.055110			
9	"	"	+.030132	+1.4125	-15.40	-13.9875
			-.227422			
			-.189282			
10	"	"	-.038140	-1.7874	-10.04	-11.8274
			-.440317			
			-.341068			
11	"	"	-.099249	-4.6524	- 5.02	- 9.6724
			-.699803			
			-.545464			
12	"	"	-.154339	-7.2348	0	- 7.2348

Table XVI (Continued)

Load at Stat.	Coef. of P_o =	$-.100020M_o$	$-\varepsilon$	X_2'' p_o^2	Coef. of ψ_o =	$-\varepsilon_2$	ψ_o	$1+\psi_o''$
0	0	0	0	0	0	0	0	1.0000
1	1.688090	-.008937	+.001765	-.0043	22.388912	0	0	1.0000
2	"	-.061106	+.012349	-.0289	"	+.037393	+.0017	1.0017
3	"	-.133900	+.027370	-.0631	"	+.115115	+.0051	1.0051
4	"	-.267607	+.056497	-.1251	"	+.380133	+.0170	1.0170
5	"	-.379374	+.081673	-.1762	"	+.652484	+.0291	1.0291
6	"	-.449083	+.099875	-.2069	"	+.894523	+.0400	1.0400
7	"	-.472700	+.106517	-.2169	"	+.990162	+.0442	1.0442
8	"	-.464801	+.109933	-.2221	"	+1.044729	+.0467	1.0467
9	"	-.152574	-.024978	-.1052	"	-1.150805	-.0514	.9486
10	"	+.193122	-.227428	-.0803	"	-4.402322	-.1966	.8034
11	"	+.502549	-.440317	+.0369	"	-7.681443	-.3431	.6569
12	"	+.781498	-.699803	+.0484	"	-11.194456	-.5000	.5000

Table XVII

Hovgaard Method--Horizontal Unit Load

Solution of Simultaneous Equations

Load at Stat.	Coef. of M_o +	Coef. of P_o =	$-.051352\varepsilon_1$	M_o	1·V	$V+M_o''$
	.10[illegible]020	1.[illegible]6[illegible]6	-.000258			
	.08[illegible]607	1.6[illegible]3690	0			
1	+.021333	0	-.000258	- .0121	.62	+ .6079
			-.002405			
			-.000057			
2	"	"	-.002348	- .1101	1.48	+ 1.3699
			-.006852			
			-.000248			
3	"	"	-.006604	- .3096	2.67	+ 2.3604
			-.024794			
			-.001924			
4	"	"	-.022870	- 1.0721	4.90	+ 3.8280
			-.060707			
			-.006730			
5	"	"	-.053977	- 2.5302	8.42	+ 5.8898
			-.127924			
			-.022306			
6	"	"	-.105618	- 4.9509	12.54	+ 7.5891
			-.208776			
			-.046387			
7	"	"	-.162389	- 7.6121	16.80	+ 9.1879
			-.313746			
			-.090740			
8	"	"	-.223006	-10.4536	21.11	+10.6564
			-.325712			
			-.090944			
9	"	"	-.225768	-10.7237	21.53	+10.8063
			-.337421			
			-.104704			
10	"	"	-.232717	-10.9088	21.84	+10.9312
			-.343781			
			-.109239			
11	"	"	-.234542	-10.9943	21.99	+10.9957
			-.346883			
			-.111682			
12	"	"	-.235201	-11.0252	22.05	+11.0248

Table XVII (Continued)

Load at Stat.	Coef. of P_o =	$-.108020H_o$	$-\varepsilon$	P_o	χ_o'' P_o-1	Coef. of Q_o =	$-\varepsilon_2$	χ_3'' Q_o
0					-1.0000	22.388912	0	0
1	1.688090	+ .001306	-.000258	+.0006	- .9994	"	0	0
2	"	+ .011889	-.002405	+.0056	- .9944	"	- .007584	-.0003
3	"	+ .033439	-.006852	+.0158	- .9843	"	- .030592	-.0014
4	"	+ .115803	-.024794	+.0539	- .9461	"	- .193647	-.0087
5	"	+ .273313	-.060707	+.1259	- .8741	"	- .539995	-.0254
6	"	+ .534798	-.127924	+.2410	- .7590	"	-1.430352	-.0677
7	"	+ .822259	-.208776	+.3634	- .6366	"	-2.[illegible]	-.[illegible]
8	"	+1.129195	-.313746	+.4831	- .5169	"	-4.285817	-.1914
9	"	+1.158371	-.325712	+.4933	- .5067	"	-4.480571	-.2001
10	"	+1.178366	-.337421	+.4982	- .5018	"	-4.668625	-.2085
11	"	+1.187607	-.343781	+.4999	- .5001	"	-4.766606	-.2129
12	"	+1.190944	-.346883	+.5000	- .5000	"	-4.808596	-.2148

In the foregoing only a vertical load has been considered. In considering a horizontal load equation (36) would be

$$M = M_o + P_o y + Q_o x - 1 \cdot y + 1 \cdot H \qquad (39)$$

where H is the vertical distance from the origin to the point of application of the load. Equation (35) would be

$$\int \frac{(1-\bar{y})}{I} ds = \frac{2E}{3}\left(\frac{H-y_o}{2I_o} + \frac{2(H-y_1)}{I_1} + \frac{(H-y_2)}{I_2} + \frac{2(H-y_3)}{I_3} + \ldots + \frac{(H-y_{12})}{2I_{12}}\right) = \frac{2E}{3}\varepsilon \qquad (40)$$

The values of ε, ε_1, and ε_2 were found for the horizontal load by the integrations shown in Table XV.

The moment, thrust, and shear obtained were the values <u>just</u> to the right of the support reactions. They differ from the values <u>just</u> to the left by the amount of the support reactions. For comparison with the values found experimentally and by the elastic center method the values to the left were desired. The conversion was made by algebraic addition of support reactions as follows:

For vertical load,	moment	1·H
	thrust	no change
	shear	1
For horizontal load,	moment	1·V
	thrust	1
	shear	no change

The computations are done in Tables XVI and XVII.

APPENDIX E

Original Data

Table XVIII
Microscope Readings

Calibration of Microscope

Read.	Ames Dial Inches	Microscope Reading Divisions	Diff.	Ames Dial Inches	Microscope Reading Divisions	Diff.
1	0	114.9	---	0	63.7	---
2	.015	195.7	80.8	.020	169.1	105.4
3	.030	276.7	81.0	.040	279.5	110.4
4	.045	360.4	83.7	.060	387.4	107.9
5	.060	440.6	80.2	.080	494.0	106.6
6	.075	521.0	80.4	.100	601.2	107.2
			406.1			537.5
Calibration Constant			0.0001847			0.0001861
1	0	77.4	---	0	77.3	---
2	.015	158.1	80.7	.020	185.7	108.4
3	.030	238.9	80.8	.040	294.2	108.5
4	.045	321.8	82.9	.060	402.8	108.6
5	.060	402.6	80.8	.080	509.8	107.0
6	.075	483.9	81.3	.100	615.9	106.1
			406.5			538.8
Calibration Constant			0.0001845			0.0001860
1	0	176.6	---	0	69.3	---
2	.020	284.3	107.7	.020	176.7	107.4
3	.040	393.5	109.2	.040	284.4	107.7
4	.060	502.1	108.6	.060	392.7	108.3
5	.080	609.8	107.7	.080	499.8	107.1
6	.100	714.5	104.7	.100	605.8	106.0
			537.9			536.5
Calibration Constant			0.000186			0.000186

Table XIX

Microscope Experimental Readings

Vertical Deflections

Stat.	Moment Read.	Moment Diff.	Thrust Read.	Thrust Diff.	Shear Read.	Shear Diff.	Stat.	Thrust Read.	Thrust Diff.
1p	521.4	---	R 421.0	---	U 598.5	---			
	406.5	114.9	W 421.5	+ .5	D 331.5	267.0			
	521.4	114.9	R 421.0	+ 1.5	U 598.6	267.1			
	407.1	114.3	W 422.0	+ 1.0	D 329.0	269.6			
	522.0	114.9	R 421.0	+ 1.0	U 597.9	268.9			
	406.5	115.5	W 423.0	+ 2.0	D 329.9	268.0			
			R 421.0	+ 2.0	U 598.2	268.3			
	Avg. =	114.9	Avg. =	1.33	Avg. =	268.1			
2p	562.8	---	W 402.0	---	U 589.9	---	2s	R 400.0	---
	348.8	214.0	R 391.5	10.5	D 321.0	268.9		W 405.0	5.0
	563.9	215.1	W 404.0	12.5	U 590.5	269.5		R 400.0	5.0
	345.7	218.2	R 390.0	14.0	D 322.0	268.5		W 405.0	5.0
	565.0	219.3	W 401.5	11.5	U 592.4	270.4			
	347.4	217.6	R 391.0	10.5	D 322.9	269.5			
	Avg. =	216.8	Avg. =	11.8	Avg. =	269.4		Avg. =	5.0
3p	421.2	---	R 395.0	---	U 549.7	---			
	111.6	309.6	W 415.0	20.0	D 278.3	271.4			
	418.9	307.3	R 395.0	20.0	U 550.5	272.2			
	110.5	308.4	W 413.0	18.0	D 279.8	270.7			
	418.5	308.0	R 398.0	15.0	U 551.6	271.8			
	112.5	306.0	W 414.0	16.0	D 278.7	272.9			
	416.9	306.4			U 548.2	269.5			
	Avg. =	307.9	Avg. =	17.8	Avg. =	271.4			
4p	366.1	---	R 195.0	---	U 312.1	---			
	-5.0	373.1	W 161.0	34.0	D 47.0	265.1			
	370.4	375.4	R 194.2	33.2	U 315.0	268.0			
	-6.0	376.4	W 159.0	35.2	D 45.0	270.0			
	369.9	375.9	R 201.0	42.0	U 317.8	272.8			
	-7.1	377.0	W 164.4	36.6	D 45.0	272.8			
	366.7	373.8	R 195.7	31.3	U 319.5	274.5			
	Avg. =	375.2	Avg. =	35.4	Avg. =	270.5			

* R or W - Indicates red (large) or white (small) plug inserted in Deep's Gage.
* U or D - Indicates left half of gage up or down relative to right half.

Table XIX (Continued)

Stat.	Moment Load.	Moment Diff.	Thrust Load.	Thrust Diff.	Shear Load.	Shear Diff.	Stat.	Thrust Load.	Thrust Diff.
5p			R 479.7	--	U 408.0	--	5s	U 316.1	--
	336.0	--	W 420.9	58.8	D 683.0	275.0		R 359.0	42.9
	755.0	419.0	R 471.3	50.4	U 405.0	278.0		W 316.2	42.8
	340.0	415.0	W 417.5	53.8	D 685.0	280.0		R 359.0	42.8
	755.0	415.0	R 472.8	55.3	U 408.5	276.5		W 316.2	42.8
	340.0	415.0	W 424.5	48.3				R 362.3	46.1
			R 475.9	51.4				U 317.0	45.3
			W 425.0	50.9					
	Avg. = 416.0		Avg. = 52.7		Avg. = 277.4			Avg. = 43.8	
6p	152.0	--	W 252.0	--	U 7 .0	--			
	583.0	431.0	R 197.5	54.5	D 378.0	285.0			
	153.0	431.0	W 251.	53.5	U 79.0	294.0			
	583.0	431.0	R 194.0	57.0	D 370.0	291.0			
	153.0	430.0	W 252.0	58.0	U 80.0	290.0			
			R 192.0	60.0					
	Avg. = 430.5		Avg. = 56.6		Avg. = 292.5				
7p	704.0	--	W 452.5	--	D 298.9	--			
	265.0	439.0	R 514.8	62.3	U 587.2	288.3			
	696.0	431.0	W 447.0	67.8	D 307.1	280.1			
	265.0	431.1	R 507.3	60.3	U 587.1	279.0			
	705.0	440.0	W 449.6	57.7	D 300.5	286.6			
	267.0	437.0	R 510.0	60.4	U 583.5	283.0			
			W 451.8	58.2					
	Avg. = 433.3		Avg. = 61.1		Avg. = 283.6				
8p	406.5	--	R 490.1	--	U 620.0	--	8s	U 406.0	--
	830.5	427.5	W 437.9	52.2	D 344.9	276.1		R 471.5	65.5
	413.6	422.4	R 492.1	55.2	U 624.0	279.1		W 408.0	65.5
	834.1	420.5	R 436.4	53.7	D 342.0	277.5		R 468.0	62.0
	831.5	420.3	R 492.1	53.6	U 624.5	279.5		W 406.7	62.1
	826.0	420.2	W 432.5	59.5	D 340.0	280.0		R 468.0	62.1
	405.0	423.0	R 484.1	51.6	U 631.0	291.0			
	Avg. = 423.3		Avg. = 54.3		Avg. = 279.5			Avg. = 63.1	

Table XIX (Continued)

Stat.	Moment Read.	Moment Diff.	Thrust	Thrust Read.	Thrust Diff.	Shear	Shear Read.	Shear Diff.	Stat.	Shear Read.	Shear Diff.
9p	569.0	---	R	360.0	---	U	373.0	---			
	182.0	387.0	W	389.0	29.0	D	636.5	263.5			
	568.0	386.0	R	355.0	34.0	U	376.0	260.5			
	181.0	387.0	W	392.0	37.0	D	629.0	253.0			
	570.0	389.0	R	360.0	32.0	U	374.0	255.0			
	186.0	384.0	W	390.0	30.0	D	620.0	255.0			
	568.0	382.0	R	360.0	30.0						
	186.0	382.0	W	392.0	32.0						
	Avg. =	385.3		Avg. =	32.0		Avg. =	257.4			
10p	520.5	---	R	467.5	---	U	575.6	---	10s	U 242.6	---
	850.0	337.2	W	475.6	8.1	D	362.1	213.5		D 194.0	48.6
	526.0	332.0	R	470.0	5.6	U	581.5	219.4		U 248.5	54.5
	853.0	327.0	W	471.0	6.0	D	364.4	217.1		D 197.5	51.0
	525.0	327.2	R	465.0	13.0	U	574.0	209.6		U 250.5	53.0
	852.5	326.7	W	466.0	1.0	D	358.0	216.0		D 205.0	45.5
	Avg. =	330.0		Avg. =	7.1		Avg. =	215.1		Avg. =	52.5
11p	334.0	---	W	234.0	---	U	381.0	---	11s	D 371	---
	598.0	264.0	R	229.5	4.5	D	555.0	174.0		U 464.8	93.8
	334.0	264.0	W	238.1	8.6	U	381.5	173.5		D 371.9	92.9
	599.5	265.5	R	227.3	10.8	D	555.0	173.5		U 466.0	94.1
	334	265.5	W	239.3	12.0	U	380.0	175.0		D 375.0	91.0
	599.5	265.5	R	230.6	8.7	D	555.0	175.0			
			W	237.3	6.7						
	Avg. =	264.9		Avg. =	8.6		Avg. =	174.2		Avg. =	93.8
12p			W	657.0	---	U	485.0	---			
	647.0	---	R	671.0	14.0	D	619.0	134.0			
	441.0	206.0	W	658.0	13.0	U	481.0	138.0			
	64[illegible].0	207.0	R	669.0	11.0	D	611.0	130.0			
	443.0	205.0	W	658.0	11.0	U	481.	130.0			
	650.0	207.0	R	670.0	12.0	D	614.0	133.0			
	447.0	203.0				U	480.	134.0			
	Avg. =	205.6		Avg. =	12.2		Avg. =	133.2			

Table XIX (Continued)
Horizontal Deflections

Stat.	Moment Read.	Moment Diff.	Thrust	Thrust Read.	Thrust Diff.	Shear	Shear Read.	Shear Diff.
1p	338.0	---	W	418.8	---	U	569.9	---
	319.0	19.0	R	691.0	272.2	D	569.0	.9
	336.0	17.0	W	418.0	273.0	U	569.3	.3
	319.0	17.0	R	661.0	---	D	568.1	1.2
	337.0	18.0	W	386.4	274.4	U	571.0	2.9
	320.	17.0	R	659.0	272.6	D	567.9	3.1
			W	386.6	272.4	U	569.0	1.1
			R	660.5	273.9			
	Avg. =	17.6		Avg. =	273.1		Avg.=	1.6
2p	217.9	---	R	481.0	---	U	465.0	---
	257.8	39.9	W	210.7	270.3	D	466.0	1.0
	219.6	38.2	R	479.9	269.2	U	465.0	1.0
	258.6	39.0	W	210.4	269.5	D	465.0	0
	219.6	39.0	R	496.0	---	U	464.0	1.0
	259.5	39.9	W	226.7	269.3	D	464.0	0
			R	496.6	269.9	U	465.0	1.0
	Avg. =	39.2		Avg. =	269.6		Avg. =	0.66
3p			R	432.0	---	U	295.5	---
	483.5	---	W	162.5	269.5	D	297.8	2.3
	412.6	70.9	R	430.0	267.5	U	295.2	2.6
	483.1	70.5	W	162.0	268.0	D	293.6	3.4
	412.5	70.6	R	430.0	268.0	U	295.3	3.3
	483.0	70.5	W	162.4	267.6	D	298.3	3.0
	413.0	70.0	R	430.8	268.4	U	297.5	.8
	Avg. =	70.6		Avg. =	268.2		Avg. =	2.6
4p	397.0	---	R	621.7	---	D	351	---
	295.5	101.5	W	362.9	258.8	U	348	3.0
	396.0	100.5	R	622.0	259.1	D	350	2.0
	295.5	102.5	W	361.0	261.0	U	348	2.0
	397.0	102.5	R	617.0	256.0	D	348	0
	295.0	103.0	W	360.0	257.0	U	348	0
			R	620.0	260.0			
	Avg. =	102.4		Avg. =	259.0		Avg. =	1.7

Stat.	Moment Read.	Moment Diff.	Shear	Shear Read.	Shear Diff.
3s	360.0	---	D	362.0	---
	366.0	6.0	U	362.0	0.0
	359.0	7.0	D	362.0	0.0
	366.0	7.0	U	361.5	.5
	359.0	7.0	D	361.5	0
	Avg. =	6.8		Avg. =	.1

Table XIX (Continued)

Stat.	Cement Read.	Cement Diff.	Thrust Read.	Thrust Diff.	Shear Read.	Shear Diff.
5p	305.0	---	L 273.0	---	U 388.0	---
	470.0	165.0	R 510.0	237.0	D 395.0	7.0
	309.5	160.5	L 273.0	237.0	U 385.0	10.0
	469.5	160.0	R 510.0	237.0	D 393.0	8.0
	309.5	160.0	L 273.0	237.0	U 387.0	6.0
	Avg. =	161.4	Avg. =	237.0	Avg. =	7.7
6p	337.0	---	L 247.0	---	D 196.0	---
	548.0	211.0	R 456.0	209.0	U 178.0	18.0
	339.0	209.0	L 248.0	208.0	D 196.0	18.0
	549.0	210.0	R 456.0	208.0	U 176.0	20.0
	338.0	211.0	L 247.5	208.5	D 196.0	20.0
			R 451.0	203.5		
	Avg. =	210.2	Avg. =	207.4	Avg. =	19.0
7p	347.8	---	L 246.3	---	D 235.2	---
	86.2	261.6	R 413.2	166.9	U 198.5	36.7
	354.5	268.3	L 253.0	160.2	D 234.0	35.5
	96.1	258.4	R 431.0	178.0	U 200.3	33.7
	351.0	254.9	L 253.1	177.9	D 231.8	31.5
	89.0	262.0	R 421.2	168.1	U 197.1	34.7
			L 254.5	166.7		
	Avg. =	261.0	Avg. =	169.6	Avg. =	34.4
8p	432.0	---	L 265.0	---	D 362.0	47.0
	135.0	297.0	R 407.0	142.0	U 309.0	53.0
	428.5	293.5	L 262.0	145.0	D 364.0	55.0
	133.0	300.5	R 408.0	146.0	U 307.0	57.0
	431.0	298.0	L 267.0	141.0	D 362.5	55.5
	137.0	294.0	R 408.0	141.0	U 310.0	52.5
	432.0	295.0				
	Avg. =	297.2	Avg. =	143.0	Avg. =	53.5

Table XIX (Continued)

Stat.	Moment Read.	Moment Diff.	Thrust	Thrust Read.	Thrust Diff.	Shear	Shear Read.	Shear Diff.	Stat.	Shear Read.	Shear Diff.
9p	555.0	---	R	348.0	---	U	365.5	---	9s	U 760.0	---
	251.0	304.0	W	208.0	142.0	D	419.0	53.5		D 816.0	56.3
	545.5	294.9	R	347.0	141.0	U	367.9	51.1		U 763.0	53.0
	255.2	290.3	W	208.0	139.0	D	426.3	58.4		D 819.0	56.0
	550.0	300.8	R	346.0	140.0	U	371.0	55.3		U 769.0	56.0
	250.0	300.0	W	206.0	140.0	D	424.0	53.0		D 816.0	53.0
	550.0	300.0	R	348.0	140.0						
			W	214.0	134.0						
	Avg. = 299.3		Avg. = 139.4			Avg. = 54.3			Avg. =55.0		
10p	486.5	---	R	355.0	---	U	269.4	---			
	187.0	299.5	W	223.1	131.2	D	324.3	54.9			
	482.5	295.5	R	366.1	144.3	U	271.0	53.3			
	175.0	307.5	W	227.8	140.3	D	331.9	60.9			
	489.0	314.0	R	374.0	146.2	U	277.0	54.9			
	184.0	305.0	W	225.5	148.5	D	323.0	46.0			
	Avg. = 304.3		Avg. = 142.1			Avg. = 54.0					
11p	421.0	--	W	302.9	---	U	543.0	---			
	724.0	303.0	R	443.6	140.7	D	600.0	57.0			
	421.0	303.0	W	303.0	140.6	U	545.0	55.0			
	731.0	310.0	R	440.6	137.6	D	602.0	57.0			
	419.0	312.0	W	304.0	136.6	U	540.0	56.0			
	724	305.0	R	440.5	136.5	D	602.0	56.0			
			W	308.0	132.5						
	Avg. = 306.6		Avg. = 137.4			Avg. = 56.2					
12p	567.0	---	W	300.0	---	D	316.5	---			
	254.0	313.0	R	451.0	151.0	U	267.7	48.8			
	567.0	313.0	W	310.0	141.0	D	330.0	62.3			
	260.0	307.0	R	445.0	135.0	U	268.1	61.9			
	567.0	307.0	W	300.0	145.0	D	331.0	62.9			
	260.0	307.0	R	439.0	139.0	U	287.8	43.2			
			W	306.0	133.0	D	348.0	60.2			
			R	437.0	131.0	U	282.0	65.2			
			W	305.0	132.0						
			R	438.0	133.0						
			W	313.0	125.0						
	Avg. = 309.4		Avg. = 136.5			Avg. = 57.8					

Appendix F

BIBLIOGRAPHY

(1) Beggs, G. E. "An Accurate Mechanical Solution of Statically Indeterminate Structures by Use of Paper Models and Special Gages," Proceedings of American Concrete Institute, Vol. 18 (1922) pp. 58-82.

(2) Bruhn, J. "The Transverse Strength of Ships," Transactions of the Institution of Naval Architects, Vol. XLIII (1901), Henry Sotheran & Co., London.

(3) Bruhn, J. "Some Points in Connection with the Transverse Strength of Ships," Transactions of the Institution of Naval Architects, Vol. XLVI (1904), Henry Sotheran & Co., London.

(4) Fife, A. H. and J. B. Wilbur Theory of Statically Indeterminate Structures McGraw-Hill Book Co., New York (1937).

(5) Hovgaard, W. Structural Design of Warships U. S. Naval Institute, Annapolis, Md. (1940).

(6) Wilbur, J. B. and C. H. Norris Elementary Structural Analysis, McGraw-Hill Book Co., New York (1948).

AUG 31 BINDERY

Thesis 12861
D15 Daniels
Stress analysis
of transverse ship
frames.

Thesis 12861
D15 Daniels
Stress analysis of
transverse ship frames.

Library
U. S. Naval Postgraduate School
Monterey, California

ARTISAN
GOLD LETTERING
AND
SMITH BINDERY
OAKLAND, CALIF.

thesD15
Stress analysis of transverse ship frame
3 2768 002 09524 2
DUDLEY KNOX LIBRARY